ESTCP
Cost and Performance Report

(ER-200834)

Geophysical Imaging for Investigating the Delivery and Distribution of Amendments in the Heterogeneous Subsurface of the F.E. Warren AFB

November 2012

ESTCP

ENVIRONMENTAL SECURITY
TECHNOLOGY CERTIFICATION PROGRAM

U.S. Department of Defense

Report Documentation Page

Form Approved
OMB No. 0704-0188

1. REPORT DATE	2. REPORT TYPE	3. DATES COVERED
NOV 2012		**00-00-2012 to 00-00-2012**

4. TITLE AND SUBTITLE	5a. CONTRACT NUMBER
Geophysical Imaging for Investigating the Delivery and Distribution of Amendments in the Heterogeneous Subsurface of the F.E. Warren AFB	5b. GRANT NUMBER
	5c. PROGRAM ELEMENT NUMBER
6. AUTHOR(S)	5d. PROJECT NUMBER
	5e. TASK NUMBER
	5f. WORK UNIT NUMBER
7. PERFORMING ORGANIZATION NAME(S) AND ADDRESS(ES) **Environmental Security Technology Certification Program (ESTCP),4800 Mark Center Drive, Suite 17D08,Alexandria,VA,22350-3605**	8. PERFORMING ORGANIZATION REPORT NUMBER
9. SPONSORING/MONITORING AGENCY NAME(S) AND ADDRESS(ES)	10. SPONSOR/MONITOR'S ACRONYM(S)
	11. SPONSOR/MONITOR'S REPORT NUMBER(S)

12. DISTRIBUTION/AVAILABILITY STATEMENT
Approved for public release; distribution unlimited

13. SUPPLEMENTARY NOTES

14. ABSTRACT

15. SUBJECT TERMS

16. SECURITY CLASSIFICATION OF:			17. LIMITATION OF ABSTRACT	18. NUMBER OF PAGES	19a. NAME OF RESPONSIBLE PERSON
a. REPORT	b. ABSTRACT	c. THIS PAGE			
unclassified	**unclassified**	**unclassified**	**Same as Report (SAR)**	**61**	

COST & PERFORMANCE REPORT
Project: ER-200834

TABLE OF CONTENTS

Page

TABLE OF CONTENTS (continued)

Page

This page left blank intentionally.

LIST OF FIGURES

Page

LIST OF TABLES

Page

ACRONYMS AND ABBREVIATIONS

1D	one-dimensional
2D	two-dimensional
3D	three-dimensional
bgs	below ground surface
CERCLA	Comprehensive Environmental Response, Compensation, and Liability Act
CASSM	continuous active source seismic monitoring
cis-1,2-DCE	*cis*-1,2-dichloroethene
CO_2	carbon dioxide
DCE	dichloroethene
DoD	Department of Defense
EAGL	Environmental and Applied Geophysics Laboratory
ERPIMS	Environmental Resources Program Information Management System
ERT	electrical resistivity tomography
ESTCP	Environmental Security Technology Certification Program
FEW	F.E. Warren Air Force Base
GIS	Geographic Information System
HRC®	Hydrogen Release Compound
IDW	investigation derived waste
ISCO	in situ chemical oxidation
LBNL	Lawrence Berkeley National Laboratory
LTM	long-term monitoring
m/s	meters per second
MCL	maximum contaminant level
mg/L	milligrams per liter
MNA	monitored natural attenuation
ORP	oxidation reduction potential
ppb	parts per billion
psig	pounds per square inch gage
P-wave	primary-wave
RA	remedial action
RAO	Remedial Action Objective

RI	Remedial Investigation
ROD	Record of Decision
ROI	radius of influence
S-wave	secondary or shear wave
SS7	Spill Site 7
USAF	U.S. Air Force
USEPA	U. S. Environmental Protection Agency
TCE	trichloroethene
TDS	total dissolved solids
TIC	total inorganic carbon
TOC	total organic carbon
trans-1,2-DCE	*trans*-1,2,-dichloroethene
VOC	volatile organic compound
VFA	volatile fatty acid
WDEQ	Wyoming Department of Environmental Quality

ACKNOWLEDGEMENTS

The authors would like to thank Mr. John Wright, Chief of Environmental Restoration, at F.E. Warren Air Force Base for his support in providing the test site for this demonstration project.

This page left blank intentionally.

EXECUTIVE SUMMARY

Engineered *in situ* treatment processes, such as *in situ* bioremediation, are being employed at many Department of Defense (DoD) installations to remediate contaminants such as volatile organic compounds (VOC) in soil and groundwater. Many of these treatment processes involve the addition of biological and/or chemical amendments into subsurface aquifers. Several delivery techniques have been developed to facilitate and increase subsurface contact between treatment materials and contaminants, including hydraulic fracturing. Although fracture-based delivery strategies are being used to increase subsurface distribution of delivered treatment materials (i.e., amendments) within tight formations, demonstrating the actual achieved distribution using conventional borehole drilling methods can be ineffective, cost prohibitive, and accompanied by high uncertainty. In particular, emplaced fractures may lead to complicated three-dimensional (3D) geometries, which can be difficult to characterize using one-dimensional (1D) (e.g., wellbore) sampling approaches. This study focused on improving the ability to develop conceptual amendment delivery models for *in situ* bioremediation and is based on the premise that geophysical imaging of amendment emplacement via hydraulic fracturing can reduce uncertainty in design and performance monitoring phases, thereby increasing efficacy and cost effectiveness of the remedial treatment.

Objectives of the Demonstration

The objectives of this Environmental Security Technology Certification Program (ESTCP) study were to (1) assess the utility of time-lapse geophysical methods for monitoring fracture development and the ability of fractures to distribute the remedial amendment, and (2) use that information together with conventional soil core and groundwater monitoring data to quantify the cost-benefit of using geophysical methods to develop an optimal delivery strategy prior to full-scale remedial action. Spill Site 7 (SS7), the location of a trichloroethene (TCE) plume at F.E. Warren Air Force Base (FEW), was used for comparison of the fracturing results for this demonstration. A remedial action (RA) involving hydraulic fracturing and *in situ* bioremediation was conducted at SS7 in 2009. A particular benefit of using SS7 as a comparison for this demonstration is that an average radius of influence (ROI) has been estimated for SS7 using conventional (wellbore-based) approaches and full-scale RA costs have been documented. Therefore, the ROI can be used to assess the potential cost-benefit of using geophysical imaging technologies for field scale implementation.

Technology Description

This study involved *in situ* bioremediation via hydraulic fracturing and the use of geophysical imaging to monitor fracture emplacement and amendment distribution. Seismic and electrical monitoring methods were the primary techniques selected for this study based on a conceptual model of geophysical detection limits of fracture and remediation processes. Laboratory studies were first conducted to confirm the conceptual models. Then a pilot study was conducted at SS7 to introduce the amendment (Hydrogen Release Compound® [HRC®]) with guar and proppant into the subsurface using hydraulic fracturing. Time-lapse electrical resistivity tomography (ERT) and seismic datasets were acquired before, during, and after fracture emplacement using both surface and crosshole-based configurations. Several seismic methods were tested, including continuous active source seismic monitoring (CASSM), which was the first-of-kind deployment for remediation monitoring. Other traditional datasets (such as groundwater contaminant

concentrations, drilling pressure and injection monitoring, surface displacement and tilt meter measurements, and drill-back validation holes) were collected and used to constrain and validate the interpretation of geophysical measurements in terms of fracture and associated system responses.

Demonstration Results

The seismic and electrical monitoring methods were found to be extremely useful in imaging fracture propagation and amendment distribution during the study. In particular, crosshole high frequency and CASSM seismic data were useful for quantifying the number and distribution of emplaced fractures, while the crosshole electrical data provided information about the distribution of amendments within and away from the fractures. A novel orbital S-wave crosswell source was also tested but technical limitations encountered during processing limited the utility of the datasets (see Appendix E of the Final Report). Analysis of the geophysical results, both individually and in combination, was performed to determine the size of the area impacted by the fractures. After 1 year of post-fracture monitoring, quarterly geophysics datasets indicated a minimum fracture ROI of 9 meters (m) (29.5 feet [ft]) with a 0.3 m (1.0 ft) vertical impact zone and an amendment distribution ROI of 5.2 m (17 ft) with a 0.8 m (2.5 ft) vertical zone distribution. The geophysical imaging also led to an updated conceptual model of fracture and amendment emplacement for the site. For example, the geophysical data suggested that the fractures and distributed amendment did not emanate radially from the fracture initiation point but were offset; the fracture radius was larger than expected, but the amendment distribution radius was smaller. Additionally, the geophysics confirmed that fractures cannot always be successfully emplaced in the subsurface, as was expected based on drilling indications.

The geophysically-obtained ROIs were used for subsequent cost-benefit analysis. To evaluate the performance, the observed ROIs were compared to a standard design ROI of 6.1 m (20 ft), which was borrowed from the analogue SS7 site at FEW. The cost-benefit analysis suggest that use of geophysical methods could lead to a 20% reduction in fracture initiation points when compared to the standard design, meeting one of the key technical objectives for this study. Future deployment of similar geophysically-based fracture assessments could follow a similar series of steps (See Figure 1); (a) a pilot fracture installation with imaging, (b) determination of geophysically-informed fracture ROI (both vertical & lateral), and (c) design of full-scale fracture treatment using determined fracture ROI constraints.

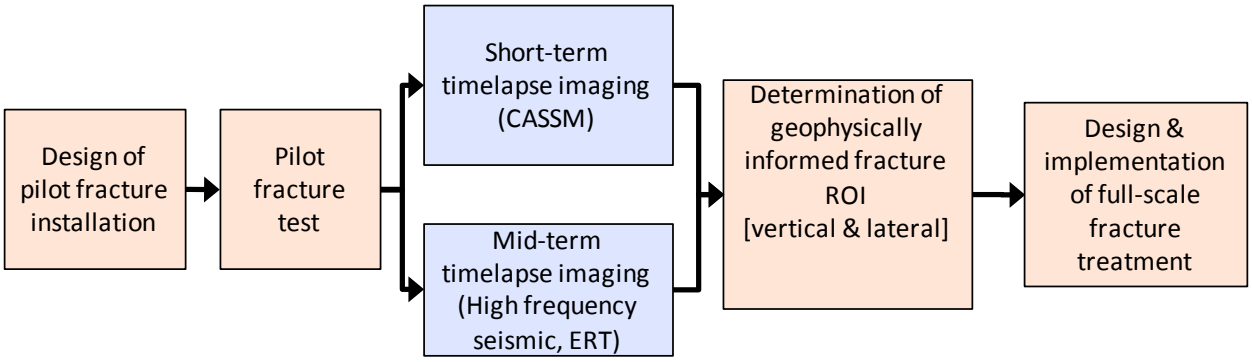

Figure 1. Using geophysics for designing fracture remediation projects.

.

Implementation Issues

Several issues could potentially impact the use of geophysical data to provide high-quality data needed to design a full-scale remedial action. The first issue is the thoughtful design of the pilot study site, which should take into consideration the propagation characteristics of the different geophysical signals, the expected fracture distribution, and the costs of drilling wellbores for geophysical data acquisition. This study found that in areas where wellbore placement resulted in good geophysical signal coverage the fracture and amendment distribution could be estimated with high confidence. However, for areas where wellbore placement resulted in poor or absent geophysical coverage, the fracture and amendment distribution could only be estimated with low confidence.

Another consideration is the role of heterogeneity on fracture propagation characteristics. This study was designed to test and image induced fracture characteristics in two different lithologies. The study illustrated that the project team was unsuccessful at installing fractures in one of the lithologies. Although these results highlight the value of geophysical monitoring for understanding fracture distribution as a function of heterogeneity, it emphasizes the need to also consider the geology carefully during pilot study and full-scale design of fracture-based treatment. Finally, procurement of the CASSM geophysical method also presents an implementation issue. The CASSM system was developed at Lawrence Berkeley National Laboratory (LBNL) and is not commercially available unlike the other geophysical methods tested. However, the fabrication of the CASSM system is not onerous and it could be built in the future by geophysical service providers.

1.0 INTRODUCTION

1.1 BACKGROUND

Engineered in situ treatment processes (such as in situ bioremediation) are being employed at many Department of Defense (DoD) installations to remediate contaminants such as volatile organic compounds (VOC) in soil and groundwater. Many of these treatment processes involve the addition of biological and/or chemical amendments into subsurface aquifers. These amendments facilitate reactions that degrade or destroy contaminants, converting them into innocuous compounds, such as carbon dioxide and water, which are nontoxic to humans and ecological systems. The efficacy of these in situ treatment processes greatly depends upon the ability to deliver amendment materials to the target contaminants. Cost of implementation and success of treatment amendment delivery is directly tied to the selected delivery strategy and the site's hydrogeological heterogeneity. Several delivery techniques have been developed to facilitate and increase subsurface contact between treatment materials and target contaminants, including hydraulic and pneumatic fracturing.

Although fracture based delivery strategies are being used to increase subsurface distribution of delivered treatment amendments within tight geological formations, demonstrating the actual achieved distribution using conventional borehole drilling methods can be both ineffective and cost prohibitive. Conceptual models of fracture and amendment distribution patterns are typically based on relatively small soil core and groundwater monitoring datasets, and therefore, are generally accompanied by high uncertainty. This uncertainty can lead to incorporation of large safety factors in full-scale remedial designs, as it is necessary to err on the conservative side when estimating parameters associated with remedial and delivery strategies (e.g., the number of injection wells, fractures, and spacing of those fractures needed to achieve remediation within a specific timeframe). With the ability to reduce design uncertainty, future remedial applications have the potential to be significantly more cost-effective.

This demonstration is based on the premise that geophysical imaging of emplacement of amendments via hydraulic fracturing can reduce the uncertainty in the design phase as well as the performance monitoring stage, thereby increasing efficacy and cost-effectiveness of the remedial treatment. The study focused on monitoring processes associated with Hydrogen Release Compound (HRC®), which is a slow release polylactate electron donor. HRC® and hydraulic fracturing were used for the remedial action (RA) at Spill Site 7 (SS7), located at F.E. Warren Air Force Base (FEW), to treat trichloroethene (TCE) and its degradation products in groundwater. The conceptual model of fracture installation used to develop the full-scale RA for SS7 is shown on Figure 1. This demonstration involved an in situ bioremediation pilot test at Plume E, a plume of TCE contaminated groundwater also at FEW, that was based upon the full-scale RA implementation at SS7. Additional information on site location, geology, hydrogeology, and contaminant distribution at FEW is provided in Section 4.

The results of this study are anticipated to be transferable to other bioremediation amendments (e.g., emulsified vegetable oils, other soluble carbon amendments, etc.) introduced using different strategies (e.g., pneumatic fracturing, traditional injection, jetting, etc.), provided that the geophysical attributes are sensitive to the injectates or their end products. Future applicability may also extend to other remedial approaches such as in situ chemical oxidation (ISCO) or in

situ chemical reduction. As such, the use of geophysical datasets to build a conceptual model of fracture imaging and amendment delivery may be applicable to other DoD sites where in situ remediation is under consideration and/or applicable. An improved model is expected to lead to improved remediation efficacy and potentially lower cost associated with treatment materials and field implementation.

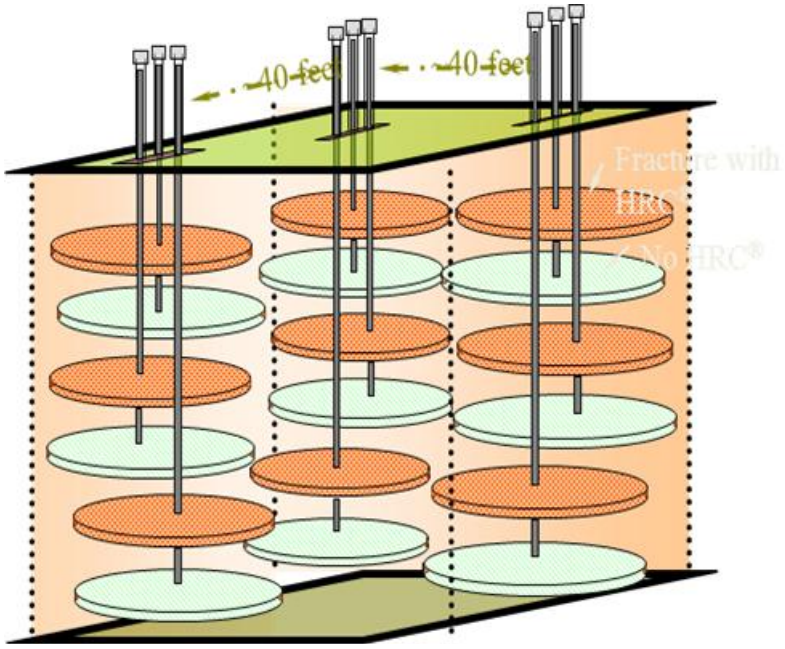

Figure 2. Conceptual fracture and amendment distribution.

For Spill Site 7, the conceptual model was that the induced fractures were distributed radially from the initiation point, with an average radius of 6.1 m (20 ft).

1.2 OBJECTIVE OF THE DEMONSTRATION

The objectives of this demonstration were to: (1) assess the utility of time-lapse geophysical methods for monitoring fracture development and ability of fractures to distribute the remedial amendment, and (2) use that information together with conventional soil core and groundwater monitoring data to quantify the cost-benefit of using geophysical methods to develop an optimal delivery strategy prior to full-scale remedial action. Seismic, radar, and electrical geophysical methods were considered for this study.

1.3 REGULATORY DRIVERS

There are no regulatory drivers specifically initiating the work included in this ESTCP project. However, FEW is a Comprehensive Environmental Response, Compensation, and Liability Act (CERCLA) site and the primary Remedial Action Objective (RAO) for SS7 and Plume E is to restore groundwater to drinking water standards (i.e., maximum contaminant levels [MCL]) for TCE and its degradation products. The target contaminants and their applicable MCLs are:

- TCE (5 micrograms per liter [µg/L]);

- *cis*-1,2-dichloroethene (*cis*-1,2-DCE) (70 µg/L);
- *trans*-1,2,-dichloroethene (*trans*-1,2-DCE) (100 µg/L); and
- Vinyl chloride (2 µg/L).

Although the regulatory drivers listed above are specific to SS7 and Plume E, these cleanup levels are typical among other DoD facilities where groundwater remediation is considered and/or RAs are implemented.

The in situ bioremediation and monitored natural attenuation (MNA) RA at SS7 is considered "in place" and "Remedy In Place" status has been approved by the Wyoming Department of Environmental Quality (WDEQ) and U.S. Environmental Protection Agency (USEPA) Region 8. Restoration will be considered fully achieved when concentrations of the target contaminants in groundwater are reduced to their respective MCLs, as indicated above.

MNA was implemented at Plume E, which also is considered to have "Remedy In Place" status by WDEQ and USEPA Region 8. This study may support the existing MNA remedy at Plume E by potentially reducing contaminant concentrations within the higher concentration areas of the intermediate groundwater zone (e.g., between approximately 13.7 and 19.8 m [45 and 65 ft] below ground surface [bgs]).

2.0 TECHNOLOGY

This study included the testing of a novel, integrated approach using time-lapse seismic, radar, and electrical attributes to monitor and detect the distribution of amendments introduced via hydraulic fracturing at Plume E. In addition to responding to in situ heterogeneity, three classes of geophysical responses are expected to be associated with the remediation strategy, as follows:

- Responses related to the initial hydraulic fracturing. It was hypothesized that fracture emplacement processes would primarily affect seismic signatures through the initial creation of fractures, pore pressure alteration, and rapid mechanical consolidation. Because seismic attributes (velocity and amplitude) are sensitive to elastic parameters and density, seismic methods were expected to be useful for monitoring fracture propagation and emplacement. In particular, it was hypothesized that the induced fractures would lead to a decrease in primary wave (P-wave) velocity and an increase in attenuation. Due to the high resolution offered by crosshole radar and its sensitivity to changes in dielectric constant associated with the geology, radar as a fracture monitoring approach was also considered. It was expected that these geophysical responses would occur almost immediately following fracture emplacement, with fracture growth occurring over minutes to hours, pore pressure dissipation occurring over similar time frames, and fracture healing occurring over a longer period depending on the plastic behavior of the geological formation.

- Responses related to amendment distribution properties within fractures and diffusion into the formation. It was hypothesized that electrical methods would be most effective at imaging initial amendment distribution within the fractures, due to its sensitivity to changes in pore fluid total dissolved solids (TDS). In particular, it was also hypothesized that the replacement of the fracture proppants with HRC® would slightly increase the electrical conductivity and the replacement of the formation pore fluid with the amendment would significantly increase the effective electrical conductivity. Given the unique dielectric signature of HRC® (Hubbard et al., 2008), we also hypothesized that radar velocity could be used to monitor the amendment distribution.

- Responses related to biogeochemical transformations associated with the treatment, potentially including guar breakdown, the long-term utilization of carbon source, and associated carbon dioxide (CO_2) bubble generation and pH changes, which could dissolve caliche in the vicinity of the injection boreholes. Because these transformations lead to changes in the pore fluid concentration, it was hypothesized that electrical methods would be the most effective remote monitoring approach; in particular, that the breakdown products would lead to an increase in bulk electrical conductivity.

In general, the conceptual model was that wave-based methods (seismic and radar) would be most effective at monitoring fracture emplacement and that electrical methods would be most effective at monitoring pore fluid geochemical changes. Due to the limitation in wellbore separation distances, and based on preliminary field testing, radar signal propagation in the field

was limited. As such, the team primarily focused on understanding and testing the seismic and electrical responses to fracture emplacement and amendment distribution. This section includes technical background for these two approaches and provides a discussion of the advantages and limitations of the focus technology guiding the development of amendment delivery conceptual models.

2.1 TECHNOLOGY DESCRIPTION

This study explored the utility of seismic and electrical methods for monitoring the distribution of induced fractures and amendments, respectively. A common time-lapse strategy was used for all methods, and two different acquisition geometries were tested. The time-lapse strategy entails collecting data before and at several time steps after the treatment (in this case, after fracture and amendment emplacement) at the same location and subtracting the baseline dataset from the subsequent datasets. This procedure removes the effect of the geology on the geophysical signature and highlights changes to the signature caused by treatment or system response to treatment (Figure 3a). Crosshole seismic, electrical, and radar datasets were collected by inserting a geophysical source into one wellbore and recording the responses at another wellbore, and repeating this process over several different wellbore depths and wellbore pairs (Figure 3b). Surface electrical datasets were collected by placing electrodes along the ground surface (Figure 3c). These methods are briefly described below.

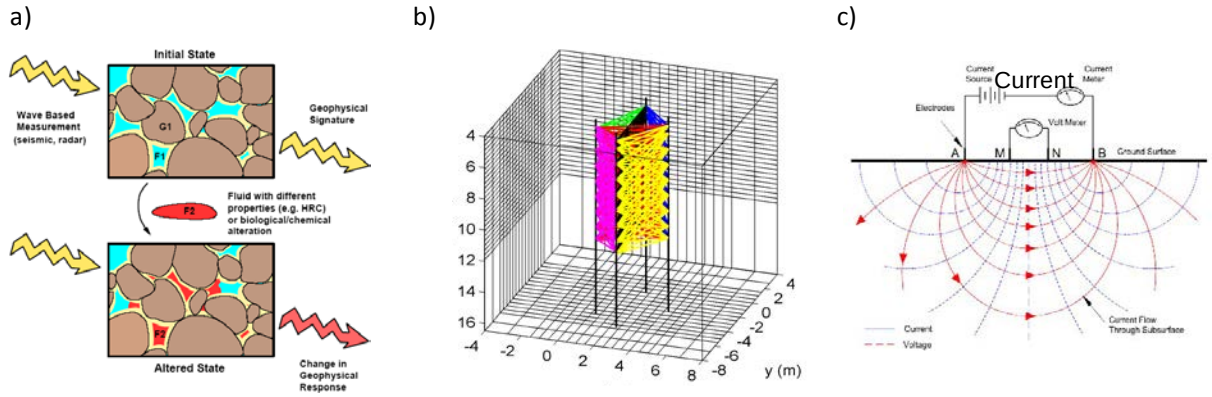

(a) Schematic showing time-lapse geophysical concept.
(b) Crosshole seismic data acquisition mode.
(c) Surface electrical data acquisition mode.

Figure 3. Data acquisition modes.

2.1.1 Seismic Methods

Seismic methods common to near subsurface investigations typically use high-frequency (approximately 100 to 5000 hertz [Hz]) pulses of acoustic energy to probe the subsurface. These pulses are generally artificially produced (using weight drop, hammers, explosives, piezoelectric transducers, etc.) and propagate outward as a series of wavefronts. The passage of the wavefront creates a motion that can be detected by a sensitive detector (geophone or hydrophone). According to the theory of elasticity upon which seismic wave propagation is based, several different waves are produced by a disturbance; these waves travel with different propagation

velocities that are governed by the elastic constants and density of the material. The P-wave energy propagates as local compression and rarefaction of a unit volume, exhibiting longitudinal particle motion in the direction of the propagating wave. Transverse waves, also called secondary or shear (S)-waves, exhibit particle motions orthogonal to the propagation direction and have lower velocities than P-waves, and therefore, arrive later in the recording. P-wave arrivals are the easiest to detect and most commonly used arrival; the focus here is exclusively on information available from P-waves.

For the seismic method, two different crosshole approaches were explored including: 1) a high frequency ("standard tomographic") approach that provides excellent spatial coverage but limited temporal resolution, and 2) a high-frequency approach that provides excellent temporal resolution but limited spatial coverage (e.g., continuous active source seismic monitoring [CASSM]). CASSM instrument fabrication and testing by Lawrence Berkeley National Laboratory (LBNL) represented firsts for environmental remediation monitoring.

The standard tomographic imaging approach entails manually placing and moving a seismic source and a string of geophones over various depth intervals within wellbores to yield dense coverage of seismic waves in the inter-wellbore area. This method yields high spatial resolution. However, since repositioning of the seismic sensor strings is manual, the datasets tend to be collected only intermittently and often with sensor positioning errors, leading to low temporal resolution. In contrast with the standard tomographic approach, the CASSM system includes: 1) an array of 10 high-frequency piezoelectric sources, which are permanently positioned within a wellbore and autonomously and sequentially activated by a high-power amplifier; and 2) two independent receiver arrays (24 and 48 levels), which can be positioned in receiving wellbores. The CASSM method geometry is illustrated in Figure 4.

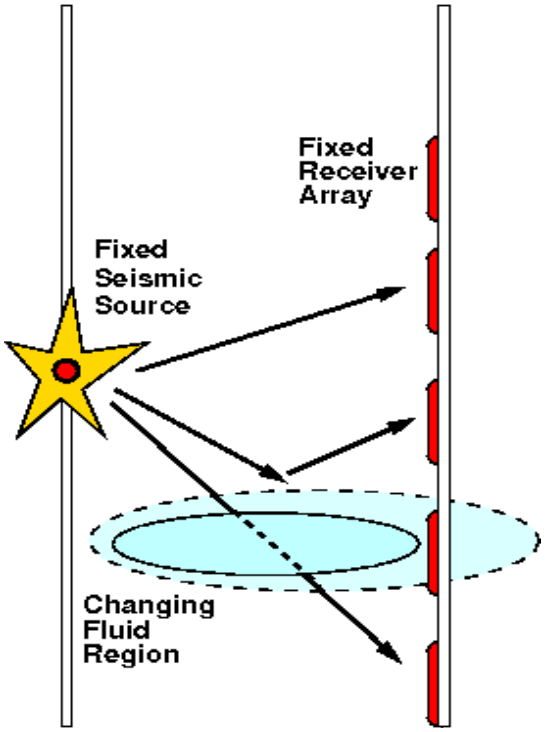

Figure 4. CASSM method geometry.

The unique aspect of the CASSM approach is that it allows highly repeatable active source seismic imaging with a fine temporal resolution; this enables the technique to autonomously and accurately image fast processes that cannot be effectively monitored using the standard tomographic seismic method. The fabricated geometry (10 sources times 72 receivers) was expected to provide sufficient data for travel time tomography along two planes that traversed the region expected to be impacted by fracturing. As each tomographic dataset can be acquired in a fully automatic mode in approximately 3 minutes, the CASSM monitoring data were expected to be able to image the fracture propagation process. Analysis of both the standard and CASSM seismic datasets includes several pre-processing steps (geometry assignment, filtering, and gain application), manual picking of the first energy arrival times, and tomographic inversion of the picked times to yield images of changes in P-wave velocity and attenuation (detailed in the following sections). Crosswell seismic imaging using an orbital shear wave source was viewed as an "opportunity" that was not identified in the original proposal; analysis of these data is still in progress and is not included in this report.

2.1.2 Electrical Resistivity Method

Electrical resistivity (the reciprocal of electrical conductivity) is an intrinsic property of a material representing its resistance to a current flow. In electrical resistivity methods, at low frequencies (<1 Hz), measured energy loss via ionic and electronic conduction dominates. Ionic conduction results from electrolytes filling interconnected pore space as well as from surface conduction via the formation of an electrical double layer at the grain-fluid interface (Revil and Glover 1997, 1998). The electrical current distribution can be visualized by equipotential surfaces, with current flow lines running perpendicular to these surfaces. Most resistivity surveys utilize a four-electrode measurement approach. The current is injected into the ground between two current electrodes, while one or more pairs of potential electrodes are used to measure electrical potential differences (or voltage). The measurement of this current and voltage, together with the geometric factor, which is a function of the particular electrode configuration and spacing, is used to calculate resistivity for uniform subsurface conditions following Ohm's law. Modern multi-channel geoelectrical equipment now includes multiplexing capabilities and automatic and autonomous computer acquisition, which greatly facilitate data acquisition within acceptable timeframes. Such surface imaging, now commonly called electrical resistivity tomography or electrical resistivity tomography (ERT), allows the electrodes (tens to hundreds) to be used alternatively as both current and potential electrodes to obtain two- or three-dimensional (2D or 3D, respectively) electrical resistivity models. For this pilot study, ERT data were collected using electrode strings fabricated at LBNL and permanently installed in the subsurface. The electrode strings were placed along the ground surface as well as in boreholes, using both 2D and 3D geometries. Electrical resistivity (the reciprocal of electrical conductivity) is an intrinsic property of a material representing its resistance to a current flow.

2.1.3 Geophysical Data Inversion, Interpretation, and Assessment

The geophysical measurements were inverted using previously developed codes to yield the following geophysical attributes: seismic velocity, seismic attenuation coefficient, radar velocity, radar attenuation coefficient, and electrical resistivity. Seismic data inversion was performed using both commercially available techniques and novel inversion techniques developed at

LBNL (Ajo-Franklin, 2007), which are specifically tailored for time-lapse analysis of injection processes. The resulting time-lapse image suites were then interpreted in terms of fracture and amendment distribution using site-specific petrophysical models that were developed based on laboratory studies conducted as part of this project (see Appendix A of the Final Report). As part of the assessment process, geophysical interpretations were compared to data collected from traditional measurements, such as groundwater and core measurements. Based on validated fracture and amendment distribution information obtained from the different geophysical methods, several acquisition scenarios were developed for the cost-benefit analysis. This included assessing how much it would cost to collect a single geophysical monitoring dataset versus suites of geophysical datasets during a pilot study relative to the respective improvements in quantifying the region impacted by fracturing, and assessing how such information and costs translated into cost savings associated with a full-scale treatment.

2.2 ADVANTAGES AND LIMITATIONS OF THE TECHNOLOGY

Physical fracture extent and general fracture characteristics are typically evaluated using conventional post-injection confirmation soil borings. The soil boring approach can be sufficient if the borings penetrate the impacted region, especially if the amendments are colored (e.g., purple potassium permanganate). For the SS7 RA, the location of fractures and the migration of byproducts associated with HRC® were difficult to assess in the field. Therefore, the fracture quantity and distribution, as well as the diffusion rates used to develop the conceptual model of HRC® distribution, were based upon observations of potassium permanganate diffusion observed at neighboring groundwater plumes where hydraulic fracturing with potassium permanganate was used as a groundwater remedy. Although such assumptions are not uncommon, they contribute to significant uncertainties in the delivery strategy conceptual model. In practice, these uncertainties often lead to higher than necessary implementation costs, as it is necessary to err on the conservative side when estimating parameters associated with the injection strategy, such as the number of injection wells or fracture zones, horizontal fracture initiation point spacing, and vertical spacing of fractures that are deemed necessary to remediate a given plume. The greatest advantage of using geophysical technologies for designing an amendment delivery strategy is that they are minimally invasive and offer excellent spatial coverage relative to conventional soil boring methods, which together facilitate an improved understanding of in situ fracture and amendment distribution. The guiding premise of this study is that the improved spatial resolution will lead to a fracture/amendment distribution model that has more certainty than soil boring- and groundwater monitoring-based models, which in turn will lead to lower overall remedial implementation costs.

There are several limitations to using geophysical datasets. The greatest limitation is that geophysical approaches provide indirect information only, such as changes in seismic velocity or electrical conductivity rather than presence of fractures or HRC® concentration; petrophysical models, either numerical or conceptual, are needed to interpret the geophysical responses to the treatment. A related limitation is that geophysical methods can be sensitive to more than one component of the experiment. For example, introduction of fractures, guar, and HRC® may all influence a geophysical attribute, and therefore, care must be taken to deconvolve the contributions. For these reasons, laboratory experiments were conducted as part of this study to gain insight into the relative contribution of different aspects of the manipulation on the

geophysical signature and potential for obtaining a unique signature of fracture zonation and HRC® distribution using multiple geophysical attributes.

The acquisition geometry and measurement support scale poses some risk to successful fracture and amendment monitoring. A general limitation of geophysical methods is that their measurement support scale is larger than the scale at which the physical or biogeochemical changes occur. Therefore, the geophysical imaging provides only an effective, or averaged geophysical response to fracturing, amendment distribution, or subsequent transformations. Geophysical averaging occurs over the support scale of the measurement, which varies with method and acquisition parameters and configuration. The time-lapse geophysical measurements were expected to be able to indicate the spatial distribution of the region impacted by fracturing and HRC® emplacement, but they were not expected to be able to image, for example, if the fracture thickness is 1/8 inch versus 1/4 inch. The wellbore geometry used to collect the geophysical data must be selected with an assumption of the induced fracture geometry. In this study, we assumed that the fractures would be distributed in a uniform disk pattern surrounding the fracture initiation point. Such assumptions can limit the utility of the geophysical data, especially if the fracture extends outside of the geophysical monitoring region.

Another limitation of using geophysical data for quantifying subsurface systems is that artifacts associated with the acquisition geometry and inversion process are often present in the final attribute image and it can be difficult to separate artifacts when interpreting subsurface heterogeneity. However, such artifacts are minimized when using time-lapse approaches (as was used in this study) because they are effectively “subtracted out” of the resulting difference image.

This page left blank intentionally.

3.0 PERFORMANCE OBJECTIVES

The quantitative and qualitative performance objectives for this study are described in Table 1.

Table 1. Performance objectives.

Performance Objective	Data Requirements	Success Criteria	Results
1. Fracture characteristics are similar in nature to those installed at SS7.	Collection of soil borings post-hydraulic fracturing.	Radii between 5.2 and 7.0 m (17 and 23 ft) from the fracture initiation location for 2000 pounds of sand delivered.	Achieved. Observed a radius between 7.0 and 7.6 m (23 and 25 ft).
2. Quantify utility of geophysical methods for delineating physical fracture and HRC® radius of distribution.	Pre- and post-fracturing geophysical datasets, laboratory analysis, inversion approaches, and confirmation soil core evaluation.	Ability to estimate mean and variance of fracture and HRC® radius as a function of heterogeneity using geophysical datasets.	Partially achieved. Different individual geophysical datasets were used to estimate the mean horizontal distribution of the fractures (between 7.0 and 9.1 m [23 and 30 ft]). Combinations of data can also be used to increase confidence in the interpretation. ERT data were used to estimate the vertical and mean radius (5.2 m [17 ft]) of injected amendment. The project team chose to use a "scenarios" approach of examining individual datasets as well as combinations of datasets rather than estimating a variance associated with a single measurement approach.
3. Assess value of different geophysical approaches for guiding development of amendment delivery strategy for quality of data collected.	• Understanding information gained from different geophysical approaches (individually and in combination) about HRC® and fracture distribution. • Understanding the risk/cost incurred in over-design (e.g., additional wells, material, and labor) and in under-design (e.g., failed treatment) of full-scale remediation treatment from project environmental engineers.	Geophysical information suggests that: a) HRC® can be adequately distributed in subsurface using 20% fewer wellbore fracture installations, thereby saving cost of over-design (labor and materials). b) Conceptual model of wellbore and fracture spacing for HRC® distribution is not adequate to ensure effective treatment (thereby saving costs/risk of remediation failure).	Achieved 20% reduction in number of fracture initiation points.

Performance Objective	Data Requirements	Success Criteria	Results
4. Cost-Benefit Analysis	• Interpretation of qualitative and quantitative performance objectives using integrated geophysical, geochemical, and soil core sample analyses. • Understanding of costs incurred using geophysical monitoring methods (acquisition, inversion, interpretation) to estimate HRC® and fracture distribution relative to costs incurred using conventional methods (e.g., groundwater sampling, core recovery) methods to estimate fracture and HRC® distribution. • Assessment of costs associated with SS7 full-scale remedial action using a design strategy based on soil core and groundwater monitoring based methods.	Total project cost savings of 20% or more for estimated full-scale remedial action implementation incorporating geophysical imaging in a field-scale pilot test to reduce design uncertainty, based on SS7 pilot test to full-scale cost relationship.	Achieved. 20% cost savings for sites greater than 4 acres and treatment zones with an ROI of 7.0 m (23 ft).
Quantitative Performance Objectives (proved by simulation)[1]			
1. Determine which geophysical method (or combination of methods) provides the best information about fracture delineation.	Estimation of fracture distribution using (a) individual geophysical methods, and (b) combined methods compared with validation coring.	Identification of single or suite of geophysical measurements that provide estimate of fracture distribution.	Achieved. Of the methods tested, the CASSM and high-frequency seismic methods provided the best information about fracture distribution. The CASSM provided the most cost-effective single monitoring approach.
2. Determine which geophysical method (or combination of methods) provides the best information about HRC® distribution.	Estimation of HRC® distribution using (a) individual methods, and (b) combined methods compared with validation wellbore data.	Identification of single or suite of geophysical measurement approaches that provide estimate of HRC® distribution.	Achieved. Crosshole, 2D ERT provided the best information about amendment distribution.
3. Determine which geophysical datasets are optimal for monitoring both fracture creation and HRC® distribution.	Estimation of HRC® and fracture distribution using (a) individual methods, and (b) combined methods compared with validation wellbore data.	Identification of single or suite of geophysical approaches that provide estimate of both HRC® and fracture distribution.	Achieved. CASSM with high-frequency seismic tomography and crosshole 2D ERT provided the best suite of methods for monitoring both fractures and amendment distribution of the methods tested.
4. Assess field-ruggedness, required user experience, and overall signal-to-noise ratio of commercially available geophysical approaches for monitoring HRC® and fracture distribution.	• Qualitative analysis of signal-to-noise ratio of electrical, high-frequency, and radar methods. • Input from geophysicists and feedback from field technicians.	Information from at least one of the imaging systems is sufficiently robust for detecting HRC® and/or fractures and is interpretable by a skilled technician.	Achieved. Time-lapse ERT acquisition and inversion approaches are commercially available and could be used by a skilled technician to estimate amendment distribution.

Notes:
ROI = radius of influence

4.0 SITE DESCRIPTION

FEW is located west of the city of Cheyenne, in south-central Laramie County in southeastern Wyoming (Figure 5). From a contaminant perspective, FEW is divided into three zones: Zone D, Zone B, and Zone C. Zone D is generally defined as the portion of FEW bounded by Roundtop Road along the western boundary of the base (Figure 6), Crow Creek to the north and east, Diamond Creek to the northwest, Zone B to the southwest, Zone C to the southeast, and Happy Jack Road along the southern boundary of the base. Zone D contains five groundwater plumes contaminated with TCE and its degradation products (i.e., *cis*-1,2-DCE, *trans*-1,2-DCE, and vinyl chloride) at concentrations exceeding federal MCLs (USAF, 2006a).

Figure 5. F.E. Warren Air Force Base site location.

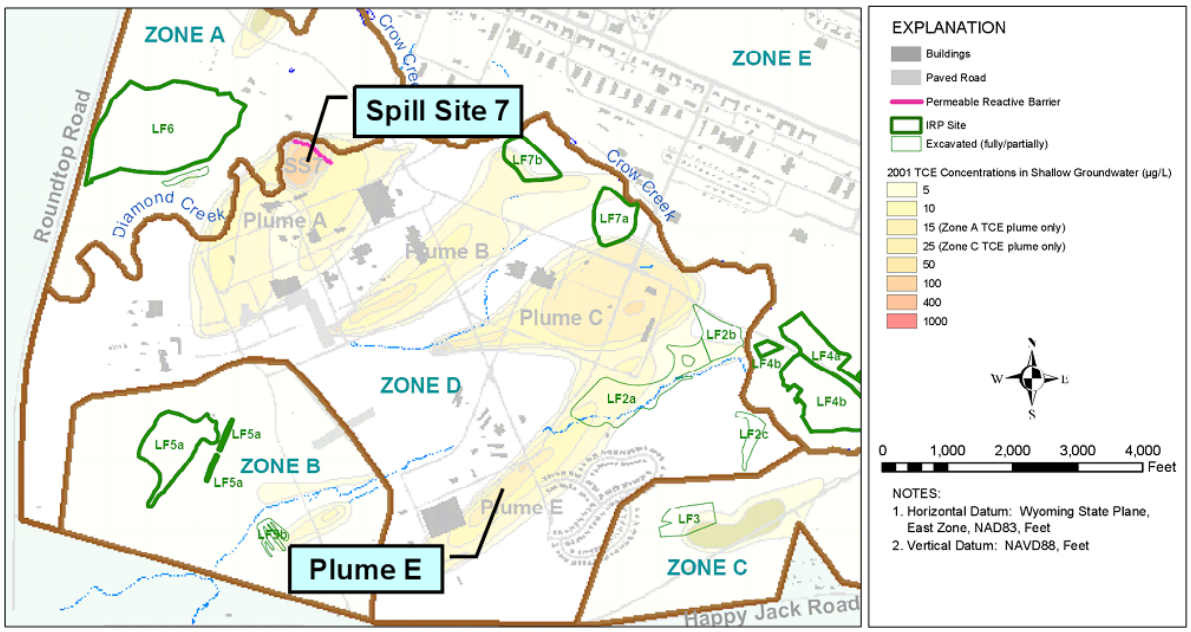

Figure 6. SS7 and Plume E within Zone D at F.E. Warren Air Force Base.

FEW was selected for this project based on three primary factors: 1) the understanding of site geology, 2) previous experience with hydraulic fracturing, and 3) quantified cost of a full-scale RA using a hydraulic fracturing and HRC® approach.

Geology at FEW is highly heterogeneous with low permeability aquifer materials throughout the installation. Although variability exists across the installation, previous investigative, remedial

design, and remedial implementation work performed across FEW allows for a comprehensive understanding of general site lithology and extent of contaminant plumes. Because of the low-permeability lithology at FEW, non-traditional amendment delivery methods have been used to implement selected groundwater remedial alternatives.

The quantity and quality of site geology and hydraulic fracturing data compiled for FEW made it a sound location choice for implementing this demonstration. One of the five TCE groundwater plumes, Plume E, was selected for this demonstration because of its lithology, available monitoring network, depth range of contaminant and lithologic data, contaminant concentrations, and lack of previous intrusive remedial activities. Primarily, intrusive pilot testing and/or hydraulic fracturing have not been implemented at Plume E; therefore, the lithology is relatively undisturbed. The lithology observed at Plume E is heterogeneous and generally representative of the lithology across FEW.

4.1 SITE LOCATION

As shown on Figure 6, TCE Plume E is located to the south of Plume C, next to the southeast boundary of Zone D. A residential area, Carlin Heights, is located on a slight hill to the southeast of Plume E. The plume originates in the vicinity of Building 945, which is located at Mule Deer and Booker Roads, and extends approximately 1525 m (5000 ft) downgradient (northeast) to Crow Creek. The demonstration was performed near the head of Plume E where TCE concentrations are generally the highest.

4.2 SITE HYDROGEOLOGY

In general, the shallow stratigraphy at FEW consists of discontinuous lenses of fine grained sand and silt. The upper 6.1 to 7.6 m (20 to 25 ft) of the shallow saturated aquifer is made up of unconsolidated terrace and alluvial deposits. Below the alluvial deposits lies the Ogallala Formation, a mixture of clay, silt, poorly sorted sand, and gravel layers. Some of the sand and gravel layers have been cemented to create discontinuous sandstone and conglomerate beds. The terrace and alluvial deposits and the upper Ogallala Formation combine to form an unconfined aquifer at the installation.

The transitions between strata in the unconfined aquifer are often subtle, with one layer grading into the next. This makes it difficult to correlate distinct hydrostratigraphic units. For this reason, a simpler method of identifying hydrostratigraphic units was developed during previous investigations and RAs at FEW, which involves dividing the shallow aquifer into separate layers according to depth below the groundwater table. Three layers were defined starting at the top of the groundwater table: Layer 1 (shallow) spans the upper 6.1 m (20 ft) of the saturated zone; Layer 2 (intermediate) extends 9.1 m (30 ft) below the bottom of Layer 1; and Layer 3 extends 12.2 m (40 ft) below the bottom of Layer 2. These layers provide the basis for the shallow, intermediate, and deep aquifer zones that are referenced in subsequent FEW reports and figures. The combined aquifer thickness is assumed to be approximately 27.4 m (90 ft).

Throughout most of the site, groundwater levels are approximately 3.0 to 6.1 m (10 to 20 ft) bgs. In the floodplain of Crow Creek and the vicinity of a small tributary (the Unnamed Tributary) that crosses a downgradient portion of the plume, depths to groundwater decrease to less than 1.5 m (5 ft). Groundwater levels are generally stable, with seasonal variations from a couple of feet up to 5 feet. These fluctuations are due to groundwater recharge from precipitation and

snowmelt. The overall stability of the groundwater potentiometric surface suggests that it represents the steady-state (i.e., long-term average) condition of the groundwater flow system.

During the Zone D Remedial Investigation (RI) (U.S. Air Foce [USAF], 2003), the horizontal hydraulic gradient for areas away from Crow Creek was calculated at 0.003 m/m (0.01 ft/ft). As groundwater flow approaches the creek, hydraulic gradients perpendicular to the creek increase to 0.018 m/m (0.06 ft/ft). This appears to be the result of the relatively low permeability of terrace deposits that flank the creek. In the Crow Creek floodplain, groundwater flow was found to change direction by almost 90 degrees to flow parallel to the creek, at a reduced gradient of approximately 0.001 m/m (0.004 ft/ft).

Vertical hydraulic gradients are apparent at several well clusters in Zone D. Most of the well clusters indicate a downward gradient, which suggests that groundwater recharge is occurring in these areas. Strong downward hydraulic gradients are present in the up-gradient reaches of Plume E. The vertical head difference is pronounced near the head of Plume E, where head differences up to 3.7 m (12 ft) have been observed in the DRMO-003 well cluster (shallow to intermediate). The downward gradient at the DRMO-003 well cluster may be indicative of vertical anisotropy.

The unconfined aquifer at FEW is heterogeneous with respect to hydraulic conductivity. Slug and pumping tests historically conducted at the installation have shown that hydraulic conductivity varies by as much as six orders of magnitude. Generally, horizontal conductivity values are highest in the shallow aquifer zone and lowest in the deep aquifer zone, a variation that is consistent with the aquifer geology. The unconfined aquifer is also anisotropic, and exhibits higher hydraulic conductivity in the principal groundwater flow direction, which is to the northeast throughout most of Zone D. Vertical hydraulic head differences observed across the study area suggest that the vertical hydraulic conductivity is smaller than the horizontal hydraulic conductivity. This is likely due to the physical layering and compaction process of alluvial deposition.

Plume E includes several well locations with relatively coarse-grained sediments in the intermediate zone aquifer. For example, the lithology at the DRMO-003 well cluster is predominantly clay and fine-grained sediments in the shallow aquifer zone, but transitions to sand and silty sand in the intermediate aquifer zone. The variation in hydraulic conductivity between the shallow clayey sediments and the intermediate sandy sediments may explain the 12 ft downward vertical gradient observed at this well cluster. Other Plume E wells contain coarser-grained sediments in the intermediate aquifer zone. These intervals of coarse-grained sediments suggest that hydraulic conductivity could be higher in the Plume E intermediate aquifer than the rest of the intermediate aquifer zone at Zone D.

Slug test data also suggest that the Plume E intermediate aquifer zone has a relatively high hydraulic conductivity. Base-wide, the geometric mean for intermediate aquifer zone slug tests was 0.09 m/day (0.30 ft/day). By comparison, two slug tests conducted at the Plume E intermediate aquifer zone had estimated hydraulic conductivity values of 1.2 and 5.5 m/day (4 and 18 ft/day) (USAF, 2003).

4.3 CONTAMINANT DISTRIBUTION

Plume E was selected as the site for the dynamic field test following an assessment of its geological and chemistry data and preliminary geophysical testing described in the Demonstration Plan (LBNL, 2010). Plume E originates in the vicinity of Building 945 (Figure 7), a former motor pool maintenance facility, and extends approximately 1,525 m (5000 ft) downgradient toward Crow Creek. The operational history of Plume E is not well known and a discrete source area was not identified for the plume during the Zone D Source Areas RI (USAF, 2006b).

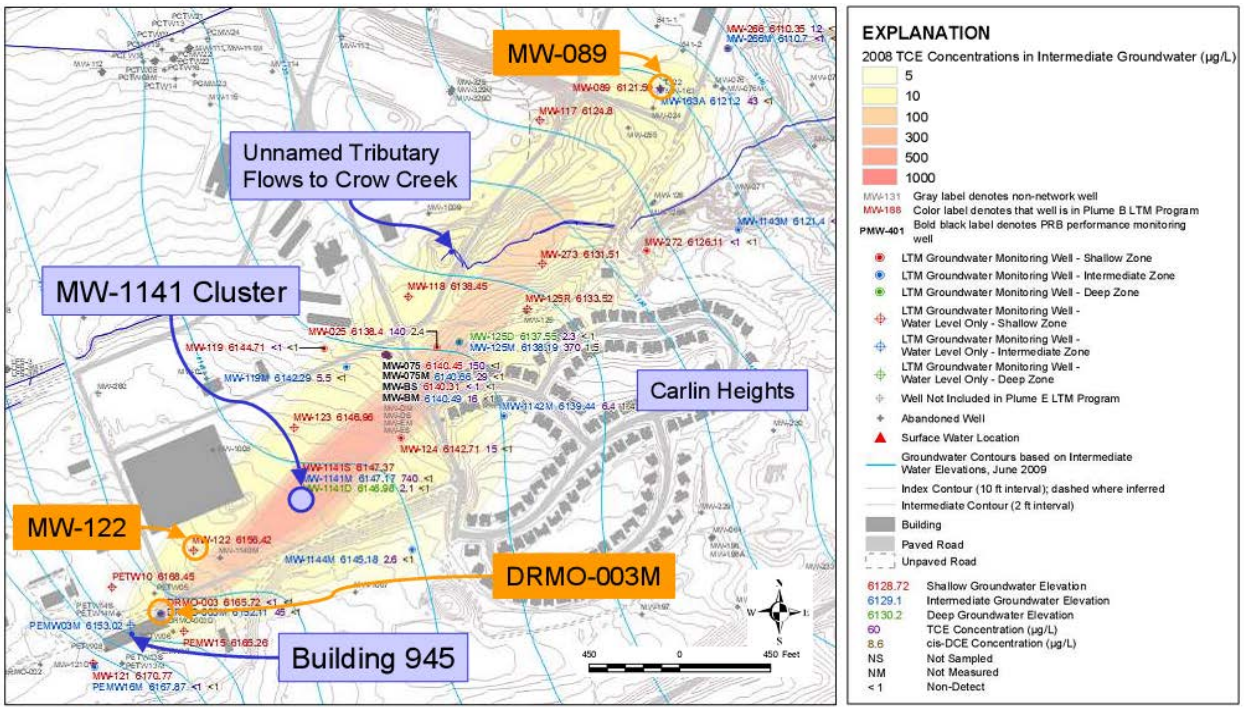

Figure 7. Plume E intermediate groundwater TCE concentration contours.

This site was selected primarily because the upper portion of Plume E does not include implemented active remedies (i.e., MNA only) and has measurable TCE concentrations, and Plume E has data for a large vertical depth range of saturated material spanning the shallow, intermediate, and deep aquifer zones, allowing multiple fracture depths and study of lithological effects.

The pilot study site is situated near monitoring well cluster MW-1141, which is located within the study area (Figure 8) and is representative of contaminant concentrations in that area. The screened intervals and example TCE concentrations for the MW-1141 well cluster are summarized below:

- The shallow aquifer zone is screened from approximately 7.3 to 10.4 m (24 to 34 ft) bgs with a TCE concentration of approximately 45 µg/L, as detected in September 2007;
- The intermediate aquifer zone is screened from approximately 15.1 to 18.1 m (49.5 ft) bgs with a TCE concentration of approximately 848 µg/L, as detected in June 2008; and

- The deep aquifer zone is screened from approximately 25 to 28 m (82 to 92 ft) bgs with a TCE concentration of approximately 4.5 µg/L, as detected in June 2008.

TCE breakdown products (i.e., *cis*-1,2-DCE, *trans*-1,2-DCE, and vinyl chloride) have not been detected within any of the aquifer zones at the MW-1141 well cluster.

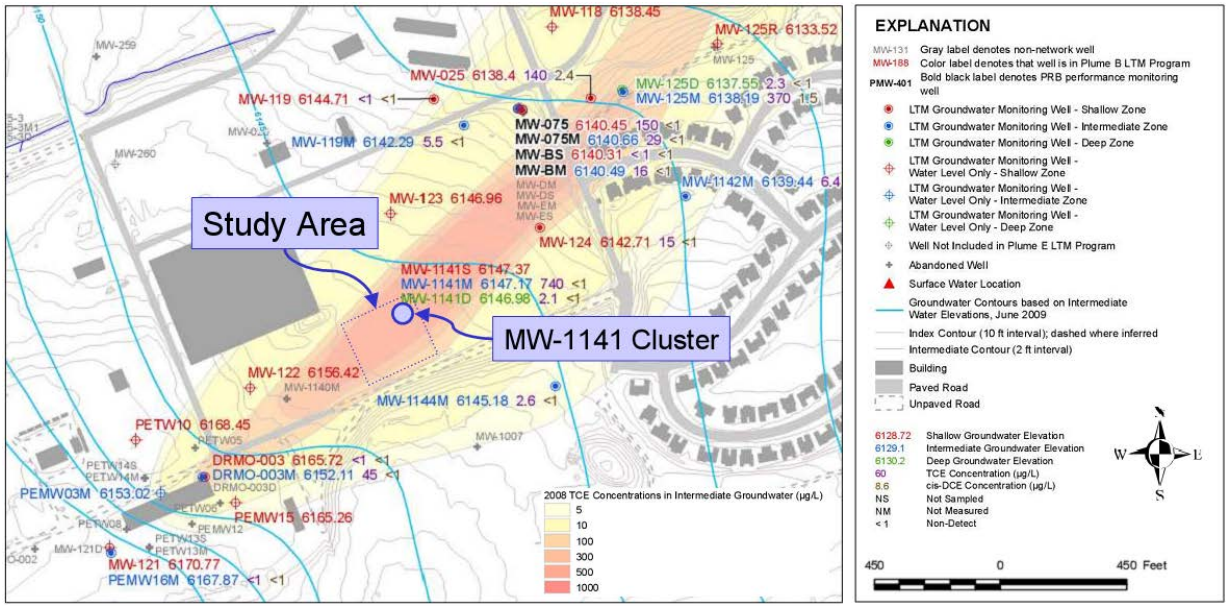

Figure 8. Plume E pilot study site.

5.0 TEST DESIGN

This section provides a detailed description of the study design and testing performed to address the quantitative and qualitative performance objectives described in Section 3. Specific activities conducted in preparation of and during the Spring 2010 dynamic pilot test are discussed below.

5.1 CONCEPTUAL TEST DESIGN

This demonstration involved an in situ bioremediation pilot test at Plume E that was based upon the full-scale RA implementation at SS7. The pilot test involved multiple tasks including: collecting and evaluating data, comparing data to the 2006 full-scale RA implementation at SS7, and performing a cost-benefit analysis.

The pilot test was performed in an untreated region of Plume E. HRC® was delivered to the subsurface via hydraulic fracturing using practices similar to those used at SS7. Fracture emplacement and delivery of HRC® was monitored using time-lapse geophysical methods as well as more conventional soil boring approaches.

The pilot test included the following key tasks:

1. installation of geophysical wellbores;
2. collection of baseline geophysical and groundwater samples for laboratory analysis;
3. installation of one hydraulic fracture within the shallow aquifer zone (i.e., Layer 1) at approximately 11.6 m (38 ft) bgs;
4. installation of one hydraulic fracture with HRC® within the intermediate aquifer zone (i.e., Layer 2) at approximately 14.3 m (47 ft) bgs; and
5. collection of post-fracturing time-lapse geophysical datasets and conventional monitoring data, including soil borings for laboratory analysis.

The pilot test enabled the exploration of field-scale geophysical responses to both fracture creation and HRC® distribution in the presence of natural heterogeneity, and therefore, permitted an assessment of the value of the technology for aiding in development of an optimal delivery strategy. Geophysically-inferred features and properties were then confirmed using secondary soil borings and core analyses in order to evaluate the performance objectives presented in Section 3 (Table 1). Further details of this dynamic pilot test are provided below.

5.2 BASELINE CHARACTERIZATION

To assist with field plan design and interpretation of geophysical data in terms of fracture and amendment distribution, several laboratory studies were performed that involved components and mixtures of components collected from the subsurface at Plume E, including: guar, HRC®, groundwater, and sediments. An environmental geophysics laboratory at LBNL was used to co-collect geochemical, hydrological, and geophysical datasets (Figure 9). Experiments were carried out at the Environmental and Applied Geophysics Laboratory (EAGL) at LBNL and included geochemical, hydrological, and geophysical datasets. Details of the laboratory experiments are

described in the Demonstration Plan (LBNL, 2010) and summarized in Appendix A of the Final Report.

Figure 9. Laboratory setup and team members, Jonathan Ajo-Franklin and Yuxin Wu.

5.2.1 Plume E Field Investigation

To provide general subsurface geology and plume location, and aid the selection of fracture locations, surface ERT surveys were conducted using an AGI SuperSting R8/IP system to select the specific location for the pilot study. Details regarding the 2009 surface ERT survey are included in the Demonstration Plan (LBNL, 2010). Results from the surface ERT data are consistent with pre-existing geochemical and lithological information and were used to help select the location of the dynamic pilot study.

5.2.2 Pilot Study Site Selection, Development, and Baseline Geophysical and Groundwater Characterization

Geophysical boreholes were installed at Plume E in October 2009 in preparation for dynamic testing planned for Spring 2010. The intentions of increasing the time between the installation of test wells and the 2010 pilot study were to: 1) allow maximum equilibrium of test wells with the native formation, 2) decrease the likelihood of surfacing via newly installed test wells, and 3) collect baseline geophysical datasets and groundwater parameters from the test wells that can be used to refine the pilot study experimental parameters, as needed.

Eleven boreholes were advanced and completed as part of baseline activities including: five ERT boreholes, five seismic boreholes with 2-inch diameter well casings, and one orbital seismic borehole with a 4-inch diameter well casing (Figure 10). Well survey coordinates are provided in Appendix B of the Final Report. Soil cores for lithologic evaluation were collected at three boreholes during the 2011 confirmation soil boring sampling event. Results are discussed further in Section 5.4. Baseline groundwater monitoring within the intermediate aquifer zone was conducted at six locations.

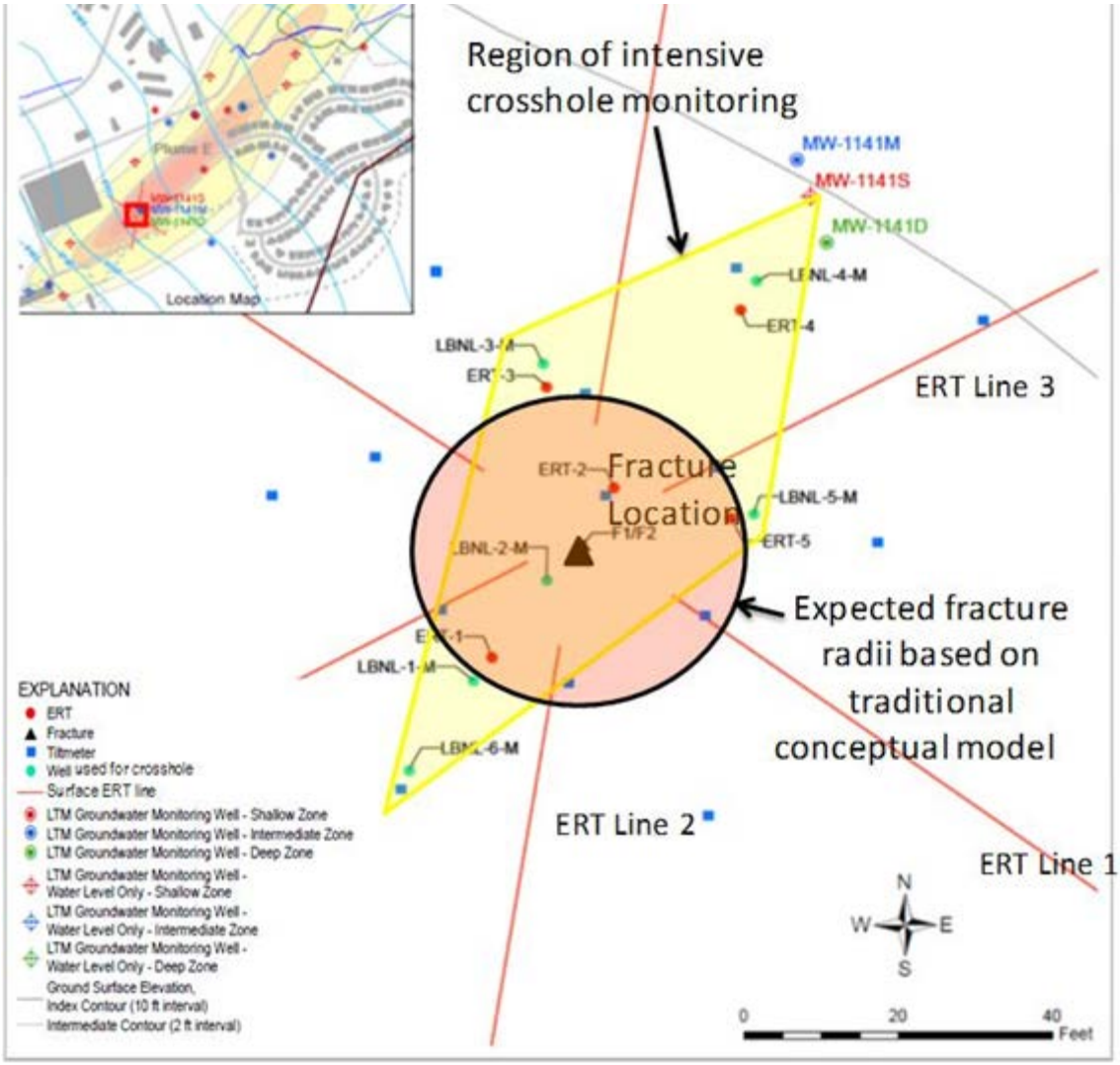

Figure 10. Pilot study layout.

Radius of influence estimated from SS7 (pink circle)
Surface ERT lines (red lines)
Crosshole imaging region (yellow diamond)
LTM = long-term monitoring

Baseline geophysical characterization, including surface and crosshole acquisition, was conducted in May 2010 to gain an understanding about the site gross hydrogeological heterogeneity and to aid in selection of the fracture location intervals. An example of surface and crosshole ERT data collected during the pilot study, as well as the two chosen intervals for introducing fractures, is shown in Figure 11.

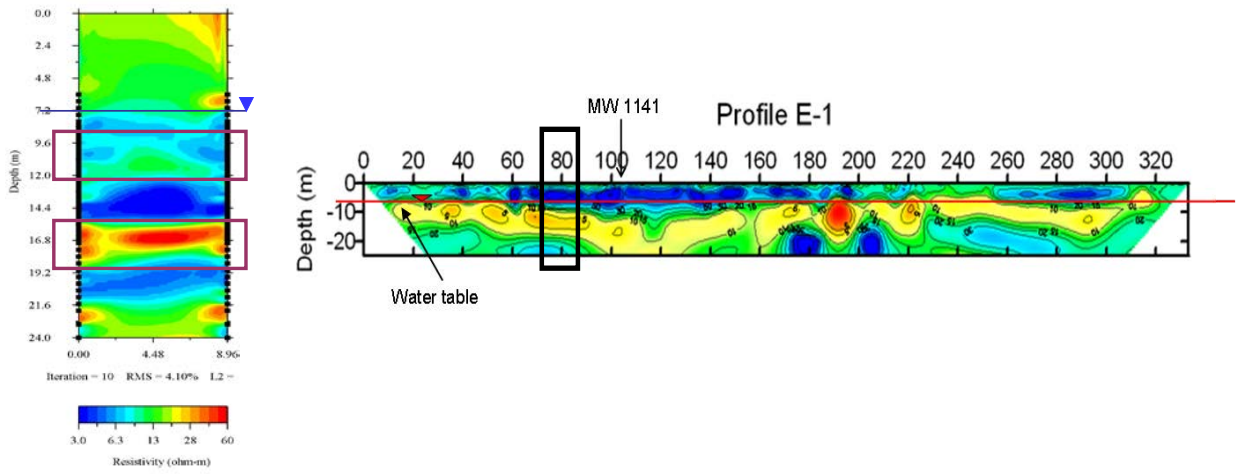

Figure 11. Examples of ERT Data

Inverted crosshole (left) and surface (right) elective resistivity tomography (ERT) data.

Baseline groundwater field parameters and samples were collected during the week of May 24, 2010. Monitoring locations included the MW-1141 well cluster as well as the four seismic wells. Groundwater parameters and laboratory analyses are included in Table 2.

Table 2. Pilot test performance groundwater parameters and laboratory analyses.

Analysis[1]	Analytical Method	Field Instrument or Laboratory Analysis	Data Use
Water-level (groundwater)	Electric tape/flume	Field	Flow direction/elevation
pH	USEPA SW-846 9040B	Field	pH values between 6 and 8 are optimal for microbial degradation
Water temperature	USEPA 170.1	Field	Microbial metabolic rates are temperature dependent
ORP	Down-well instrument	Field	Less than –100 millivolts indicates strong anaerobic conditions have been established
Dissolved oxygen	Flow-through cell	Field	Concentrations <1 mg/L indicate anaerobic processes
Specific conductance	USEPA SW-846 9050A	Field	General water quality parameter
Turbidity (groundwater)	USEPA 180.1	Field	General water quality parameter
TCE	USEPA SW-846 8260B	Laboratory	Existing target contaminant; performance monitoring
Total 1,2-DCE	USEPA SW-846 8260B	Laboratory	Not previously detected; indicates partial degradation
trans-1,2-DCE	USEPA SW-846 8260B	Laboratory	Not previously detected; indicates partial degradation
cis-1,2-DCE	USEPA SW-846 8260B	Laboratory	Not previously detected; indicates partial degradation
Vinyl Chloride	USEPA SW-846 8260B	Laboratory	Not previously detected; indicates partial degradation
Anions[3]	USEPA SW-9056	Laboratory	Performance monitoring

[1] To optimize conditions for additional biostimulation and, if necessary, bioaugmentation, additional samples may be collected for total organic carbon (TOC), total and dissolved iron, ammonia, ortho-phosphate, volatile fatty

acids (VFAs), sulfide and methane on an as needed basis based on monitoring data collected from previoussampling events.
[2] Including ethene and methane.
[3] Anions may include analyses for nitrate, phosphate, and sulfate.
mg/L = milligrams per liter
DCE = dichloroethene
ORP = oxidation reduction potential

5.3 PILOT STUDY

Implementation of the in situ bioremediation pilot study at Plume E involved several field activities, which have been grouped into four phases and are discussed below.

5.3.1 Phase 1 – Site Preparation Activities

Site preparation activities included: 1) identifying and securing existing site features, such as monitoring wells, that were potential surface conduits for fracturing materials; 2) conducting baseline groundwater monitoring to verify current (i.e., pre-fracturing) site conditions (see Table 2); and 3) mobilizing personnel, materials, and equipment to the test site.

5.3.2 Phase 2 – Fracturing and HRC® Emplacement Activities

Field activities conducted for hydraulic fracturing and HRC® emplacement are described below.

5.3.2.1 Fracture Initiation Borehole Drilling

To create each fracture initiation location, a borehole was advanced from ground surface using solid stem augers attached to a dual capability direct push drill rig. The augers were advanced to at least 0.61 m (2 ft) above the shallowest targeted fracture depth, and then removed from the borehole. Using direct push drilling methods, 2-inch diameter temporary fracture casing (e.g., direct push rod approximately 2-inches outer diameter) was driven the remaining vertical distance to reach the first target fracture depth, creating the seal necessary for horizontal fracture initiation. When the target fracturing depth was reached, the casing was retracted to expose a 2-inch vertical section of open borehole. The fracture location was then notched to prepare the borehole for fracture initiation and propagation, further described in Section 5.3.2.3 (Injection Well Installation and Completion). After the propagation of each fracture, direct push drilling resumed until the next target fracture depth was reached.

5.3.2.2 Fracture Propagation

To initiate fractures, a down-hole notching tool was inserted into the fracture initiation borehole. Notching was used to prepare the borehole for fracturing by creating a horizontal void space in the formation at the target fracture depth. This void space promotes fracture propagation in a horizontal direction during fracture initiation. The notching process is performed using a high-pressure (e.g., approximately 3500 pounds per square inch gage [psig]) water jet, and produces minimal quantities of both water and soil wastes.

The pressure at the notched area is increased until the formation “breaks” or allows initiation of the fracture. This effect was observed to occur at approximately 150 to 300 psig during previous fracturing work in other areas at FEW. Fractures were hydraulically installed into the shallow

aquifer zone (approximately 11.5 m [38 ft] bgs) and the intermediate aquifer zone (approximately 14.3 m [47 ft] bgs). For each location, we attempted to deliver 2000 pounds of sand in a linked guar carrier with approximately 200 pounds of dyed HRC®. Sand, guar, and HRC® injection mass were manually recorded during emplacement to provide additional timing information for observed phenomenon. Photographs of the various aspects of the pilot study implementation are shown in Figure 12.

5.3.2.3 Injection Well Installation and Completion

Fracture initiation boreholes were completed as injection wells for the possible subsequent injection of microbial culture for bioaugmentation. Based upon previous work performed at FEW, the 1¾-inch injection wells were installed with one 1.5-m (5-ft) screen to access the emplaced fractures (e.g., one 1.5-m [5-ft] screen per fracture).

5.3.3 Phase 3 – Performance Monitoring Activities

Performance monitoring was conducted to evaluate aquifer redox conditions following fracturing activities, as described in the subsections below.

5.3.3.1 Groundwater Monitoring

Three months after electron donor emplacement, groundwater samples were collected from the performance monitoring well locations summarized in Table 3. The purpose of the performance groundwater monitoring was to evaluate initial reductions in contaminant levels. Due to the site geology, the intermediate aquifer zone fracture did not propagate at the target depth. As a result, the groundwater well screen interval (installed prior to the pilot study) was 0.9 m (3 ft) below the fracture zone. The field parameter and analytical data collected in July 2010 confirmed that the physical separation distance between the fractured zone and the well screen interval was too large to correlate, and therefore, data were inconclusive. For this reason, subsequent groundwater performance monitoring samples were not collected.

5.3.3.2 Post-Fracture Geophysical Monitoring

Post-fracturing geophysical response datasets were collected and processed during four events following the pilot study.

The different types of data that were collected over time in association with the pilot study are depicted in Table 4. In general, the standard seismic tomographic data and all of the crosshole and surface ERT were acquired along 10 cross-sections at specific time intervals over a 6-month period before, during, and after fracturing and injection of the HRC®. Over 1000 CASSM crosshole datasets with a time-resolution of approximately 3 minutes were acquired between three wells over a 9-day period; the CASSM dataset spanned a baseline period, the fracturing events, and several days after the last fracture to allow monitoring of any fast consolidation processes that might be present.

Figure 12. Pilot Study at FEW.

1. Lawrence Berkley National Laboratory field acquisition truck at site
2. ERT data acquisition
3. Seismic data quality control analysis
4. Mixing dye for fracture identification
5. High-frequency piezo source
6. Adding dye to proppant
7. Drilling borehole at fracture location
8. ERT well layout
9. CASSM well layout

Table 3. Groundwater sample collection summary.

Sample ID	Analyte(s) and Laboratory Method				
	VOCs (SW8260B)	Dissolved Metals (SW6010B)	Alkalinity (A2320)	Anions (SW9056A)	TOC/TIC (SW9060)
Baseline Groundwater Sampling – December 2009					
LBNL-2-M	X	X	X	X	X
LBNL-3-M	X				
LBNL-4-M	X				
LBNL-6-M	X	X	X	X	X
MW-1141D	X				
MW-1141M	X	X	X	X	X
MS-1141S	X	X	X	X	X
Performance Groundwater Monitoring – July 2010					
LBNL-2-M	X	X	X	X	X/X
LBNL-4-M	X	X	X	X	X/X
LBNL-5-M	X	X	X	X	X/X

TOC/TIC = total organic carbon/total inorganic carbon

Table 4. Geophysical acquisition times.

Date	CASSM	Crosshole Seismic	Crosshole ERT	Crosshole 3D ERT	Surface ERT
May 24-28, 2010 (Baseline [Pre-Fracturing])	Begin May 28, 2010	All well pairs collected	All well pairs collected	Both 3D configurations collected	All three lines collected
June 1-3, 2010 (During Fracturing)	End June 5, 2010		Some well pairs collected	Both 3D configurations collected	All three lines collected
June 4-6, 2010 (Post-Fracturing)		All well pairs collected	All well pairs collected	Both 3D configurations collected	All three lines collected
June 8-10, 2010		All well pairs collected	All well pairs collected	Both 3D configurations collected	All three lines collected
August 26-28, 2010		All well pairs collected	All well pairs collected	Both 3D configurations collected	All three lines collected
October 13-15, 2010		All well pairs collected	All well pairs collected		All three lines collected

In addition to geophysical monitoring, three supporting datasets were acquired during the pilot study: (1) a ground deformation network was established and surface displacement was measured using uplift stakes and a total station, (2) a network of tilt sensors was co-located with the 13 displacement stakes, and (3) injection pressure and flow rate were measured to provide basic constraints on fracture initiation and propagation as well as pressure diffusion after shut-in. Pressure gauges at the fracture well head and the pump were installed and recorded automatically during emplacement of both fractures. Results of the geophysical monitoring are discussed further in Section 5.4.2.

5.3.4 Phase 4 – Demobilization Activities

Demobilization field activities conducted after hydraulic fracturing and in situ bioremediation activities included borehole abandonment and surveying. Survey data are included in Appendix B of the Final Report.

5.4 INTERPRETATION AND VALIDATION

Groundwater data, geophysical data, and validation wells were used to interpret the extent of both the fractures and amendment.

5.4.1 Groundwater Monitoring

One round of post-fracturing performance monitoring was conducted in July 2010. Three locations were sampled and analyzed for the analytes listed in Table 3. As discussed in Section 5.3.3.1, due to an inability to install the intermediate aquifer zone fracture at the target depth, the intermediate well screens were installed 0.9 m (3 ft) below the fracture zone, and the vertical separation between the fracture zone and the well screens was too large to correlate the data with potential contaminant reductions relating to the treatment. Although well LBNL-2-M did show some reduction in TCE between baseline (980 µg/L) and the July 2010 post-emplacement performance monitoring (630 µg/L), in general the results were inconclusive with respect to potential contaminant reduction from the amendment emplacement. Results for wells LBNL 4 M showed a slightly increasing TCE concentration and LBNL-5-M did not have a corresponding baseline. Results from the baseline (December 2009) and post-fracturing (July 2010) groundwater monitoring events are included in Appendix C of the Final Report.

5.4.2 Geophysical Monitoring

All geophysical data collected after the fracture initiation began were differenced from the baseline datasets to obtain changes in seismic velocity, seismic attenuation, radar velocity, and electrical conductivity. Due to the wellbore separation distances and electrical conductivity of the subsurface, the radar signal was attenuated, and therefore, the signal-to-noise ratio was not high enough to interpret. Only the seismic and electrical monitoring datasets and their joint interpretation are described herein.

We found that the CASSM allowed for accurate, autonomous, and rapid monitoring of subsurface response to hydraulic fracturing. One advantage of the autonomous acquisition process is that no manual repositioning of sources or receivers is required; the static nature of the geometry guarantees excellent signal repeatability, which simplifies extraction of subsurface changes. The changes in seismic velocity over time between two wellbores as a fracture is initiated nearby and as it propagates into the imaging plane are illustrated in Figure 13. The decrease in velocity is what is expected as the rock loses strength, or becomes fractured. The change in velocity estimated using the CASSM approach along two imaging planes, which have been unfolded from 3 to 2 dimensions for enhanced visualization is shown in Figure 14. Both of these figures show a clear decrease in velocity at approximately 12 m (39 ft) bgs, which closely matches the fracture initiation depth recorded in the drilling log.

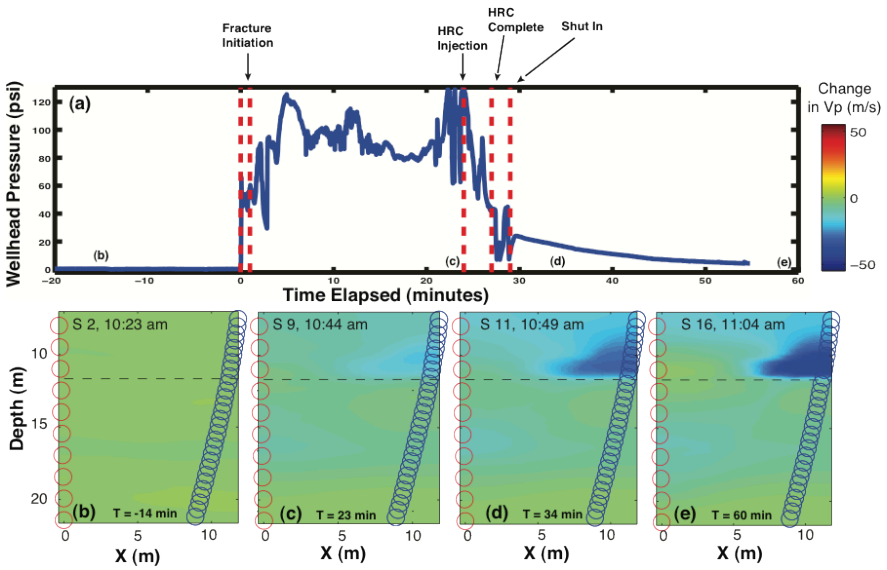

Figure 13. Wellhead pressure log.

Differential P-wave tomograms (a) during fracturing and (b) showing baseline state. Three subsequent images during and after fracture emplacement (c, d, e). On the bottom set of figures: the red circles denote source locations in well 1M, the blue circles indicate receiver locations, and the horizontal line is extrapolated from the depth at which fractures were found in a nearby validation well.

The high-resolution crosswell seismic velocity tomograms also revealed that there was an immediate decline in seismic velocity and that these data could be used to map the location and extent of the induced fractures. The change in seismic velocity along three transects 1 week after fracture installation using the standard tomographic seismic approach is shown in Figure 15. As with the CASSM imaging, the standard seismic tomographic data revealed the presence of an interpreted fracture associated with the shallow installation, but not with the deeper fracture.

To evaluate the accuracy of both standard tomographic and CASSM for monitoring fracture emplacement, it is necessary to compare the geophysical responses with each other and with direct measurements of the fracture locations. The change in velocity due to the fracturing, obtained from the standard and CASSM seismic approaches, is shown in Figure 16. The oval indicates the location of the largest velocity anomaly, which indicates a decrease in velocity over time. The dashed line is a horizontal extrapolation of the base of an induced fracture, as identified from core samples retrieved from the borehole (drill back validation holes are described below). Data in Figure 16 illustrates that while both high resolution seismic methods were able to accurately image the location of the induced fracture (which is the ultimate goal of the project), the CASSM detection of the fracture location was superior due to high repeatability and low error (the latter was largely associated with stationary sensor positioning within the wellbore). However, the standard seismic tomograms provided higher spatial resolution and more spatial coverage compared to CASSM, and because they were collected over a longer period of time, also revealed fracture “healing” (not shown).

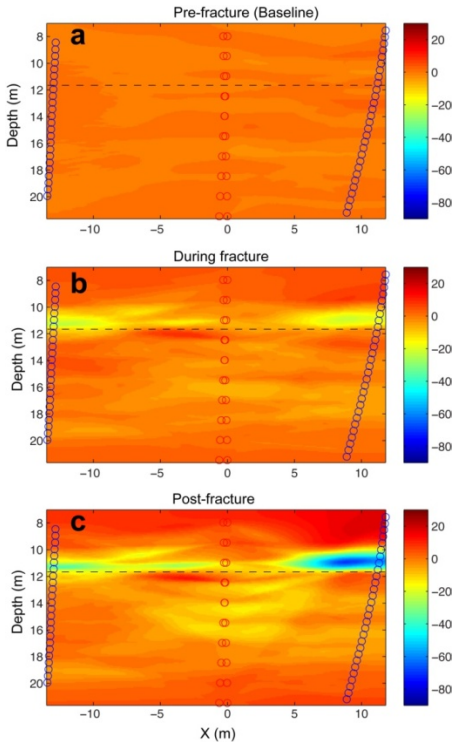

Figure 14. Results of the integrated ML-continuous active seismic monitoring inversion process.

(a) Spanning from the baseline state, (b) during the fracture process, and (c) the post-fracture state (c). The fracture is visible as a horizontal low-velocity feature at approximately 12 m (39 ft) bgs. The dashed horizontal line is extrapolated from the depth at which fractures were found in a nearby validation well. Velocity scale is meters per second (m/s) of change.

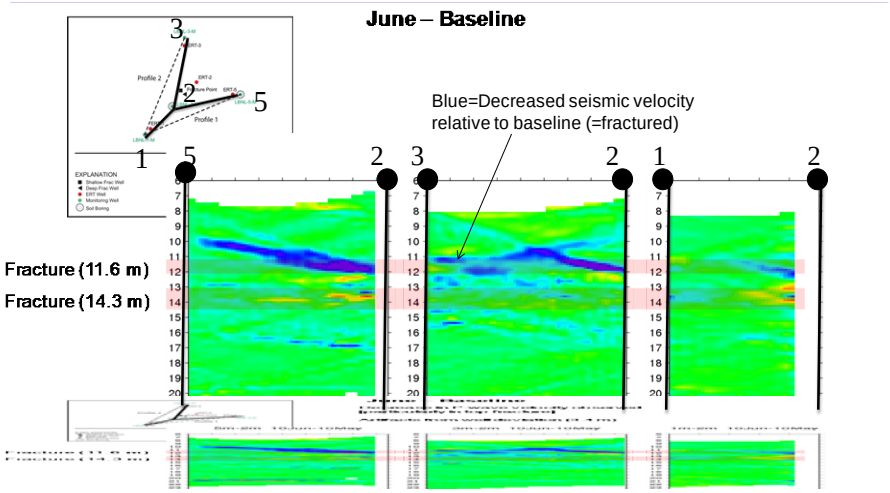

Figure 15. Change in seismic velocity.

One week after fracture installation along three transects obtained using standard seismic tomographic approach.

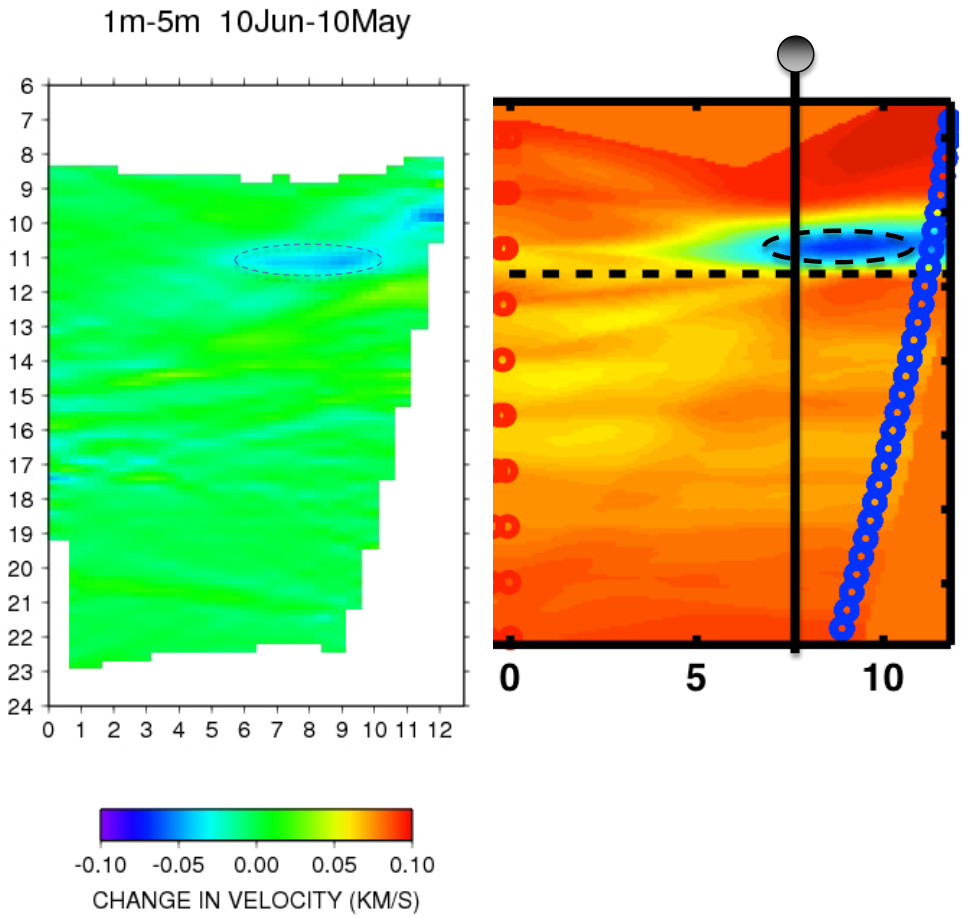

Figure 16. Relative resolution of seismic methods.

For imaging fractures based on change in velocity one day after fracturing. The standard acquisition inversion is on left, CASSM inversion on right. The dashed horizontal line is extrapolated from the depth at which fractures were found in the validation well shown on the CASSM transect. The color scale for the figure on the right is identical to that used in Figure 13.

An increase in electrical conductivity was observed in conjunction with both the shallower and deeper fracture over time. An example of these changes along a 2D ERT cross section is shown in Figure 17 and an example using a 3D grid is shown in Figure 18.

The greatest change in electrical conductivity occurred in the fractured region 2-3 months after fracturing. This delay in electrical response is consistent with the laboratory findings, where electrical conductivity increased most dramatically after breakdown of the guar. The 10-15% conductivity increase (resistivity decrease) in the shallower depth is also consistent with the core analysis described above. The change in conductivity in the deeper fracture indicates that while a complete fracture was likely not installed at this depth (as indicated by seismic and core), some porosity enhancement was produced by fracturing, which permitted the introduction of some amendment into the subsurface section.

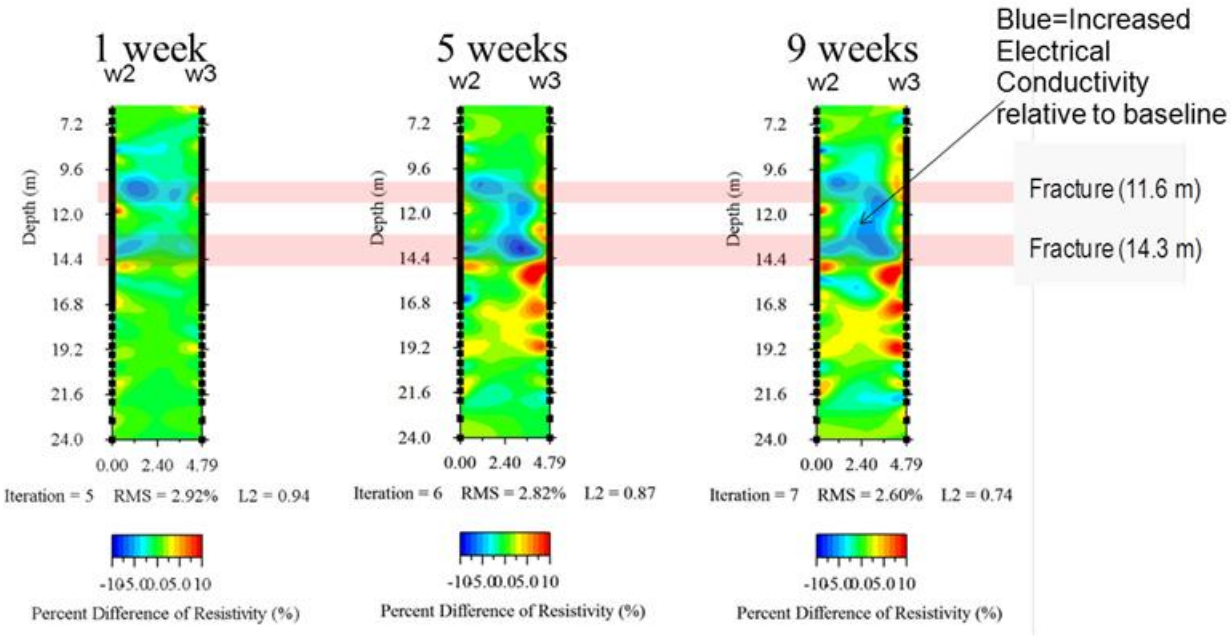

Figure 17. Changes in electrical resistivity using 2D ERT.

Changes in electrical resistivity shown along the W2-W3 2D ERT cross-section at three different acquisition times after fracture installation.

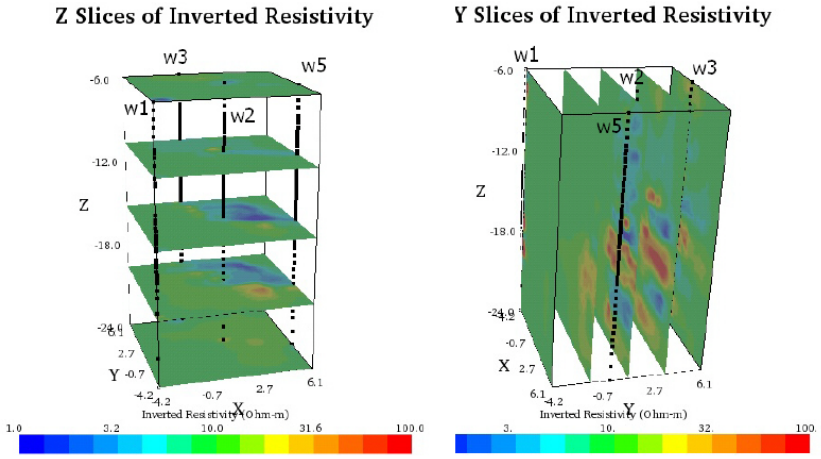

Figure 18. Changes in electrical resistivity using a 3D ERT grid.

Changes in electrical resistivity shown along 3D ERT.

The crosshole electrical data were useful for identifying distribution of the amendment injected within the induced fracture(s). These data showed that the radius of distribution of the geophysically-detectable injected amendment in the shallow fracture was substantially smaller than the fracture distribution itself. The ERT data also suggested that some amendment was injected into the deeper fracture initiation point, even if installation of a spatially extensive fracture was not successful. All data showed that the disturbed zone (through fracture creation or

amendment injection) was offset from the fracture initiation point. We found that the 3D ERT data, which required substantially greater acquisition and inversion effort, did not add substantial value to interpretation of amendment distribution. Additionally, although surface ERT measurements were useful in delineating gross hydrogeological heterogeneities (e.g., water table, lithological units), the time-lapse surface ERT data were not useful for monitoring amendment distribution associated with fracturing due to the lower resolution nature of the measurements and also because other factors (e.g., moisture changes in the shallower section due to rainfall) contributed to the geophysical responses over time.

5.4.3 Confirmation Soil Boring Drilling and Core Analysis

Four confirmation soil borings were drilled near the fracture initiation point after fracture emplacement to evaluate if the fracture characteristics (e.g., fracture thickness and approximate extent) and amendment distribution assumed for the design were attained. These soil borings were collected in May 2011, approximately 1 year after fracture initiation.

Observations of the soil borings indicated the presence of fracture sand at location LBNL-2011-SB04 at approximately 10.7 m (35 ft) bgs, which correlates well with the shallow target depth. Location LBNL-2011-SB04 is approximately 8.8 m (29 ft) from the fracture initiation point (Figure 19). Odor and the presence of a pink/orange coloration were also observed at approximately 11 m (36 ft) bgs indicating the potential presence of amendment. Reddish striations were observed at soil boring location LBNL-2011-SB02 at a depth of approximately 11 m (36 ft) bgs. Fracture sand and odor were not observed at that location. Soil boring location LBNL-2011-SB02 is approximately 5.2 m (17 ft) from the fracture initiation point. Fracture sand and coloration were observed at soil boring location LBNL-2011-SB01 at approximately 11.9 m (39 ft) and 12.5 m (41 ft) bgs, respectively. Coloration was also observed at approximately 15.8 m (52 ft) bgs; however, no fracture sand was noted. This depth is slightly deeper than the intermediate target depth and is the only indication of potential fracture propagation and amendment distribution. Location LBNL-2011-SB01 is approximately 3.0 m (10 ft) from the fracture initiation point. Soil boring LBNL-2011-SB03 was cored but not logged. Overall, the 2011 confirmation soil boring data indicated a potential fracture ROI up to 7.6 m (25 ft). Soil boring observations were recorded and are summarized in Appendix D of the Final Report.

Analysis of the core data suggests that geology may have impacted fracture propagation. According to the soil borings, fractures tended to propagate further in stiffer, more brittle clays as observed in the shallow groundwater zone near LBNL-2011-SB04. However, fracture propagation appeared to be inhibited by highly plastic, silty, clayey materials observed in the intermediate depths. It is assumed that the fracture propagated up into the shallow zone fracture following a path of least resistance.

To help understand the diffusion process of the injected amendment into the formation following fracture installation, sediment samples were collected from 6 inches above and below the fractures at both SB01 and SB03 for TOC analysis using a Shimazu TIC/TOC analyzer at LBNL. Subsamples were taken for every 1/2 inch for the first 2 inches and then every inch for another 4 inches both above and below the fracture aperture. For SB03, the fracture sand itself was also sampled due to its abundance. The sampling locations and concentrations of TOC for SB03 are shown in Figure 19. TOC concentrations are below the detection limit (<0.002%) for most samples from SB01, while detectable amounts of TOC were measured from samples from SB03. Compared to SB03, where fracture is apparent and large (Figure 19), only a thin fracture line was

identified for SB01, indicating this may be the distal end of the fracture with limited organic carbon content. This is consistent with geophysical estimation of the fracture extension shown in Figure 20.

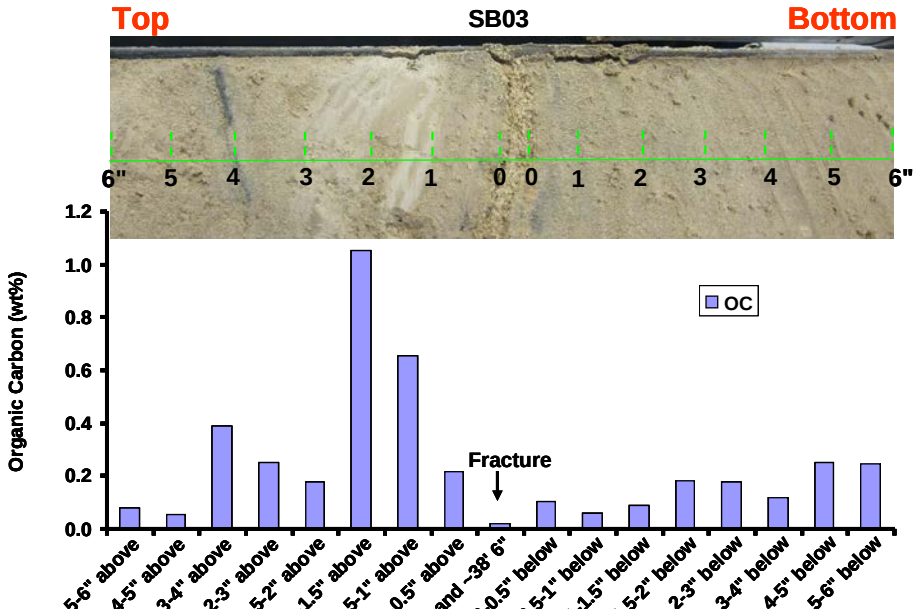

Figure 19. Total organic carbon in soils 6 inches above and below the fracture (soil bore SB03).

As shown in Figure 19, TOC concentrations range from 0.06 to 1% for soil samples from above and below the fracture and TOC concentration for the fraction sand itself is at 0.02%. The low TOC concentration of the fracture sand indicates the diffusion of organic carbon into the formations. While quantitative evaluation of the diffusion cannot be obtained because of the lack of measured background organic carbon concentrations in the soil before fracture installation and HRC® injection, TOC concentrations from soils above and below the fracture indicate the occurrence of diffusion following initial injection.

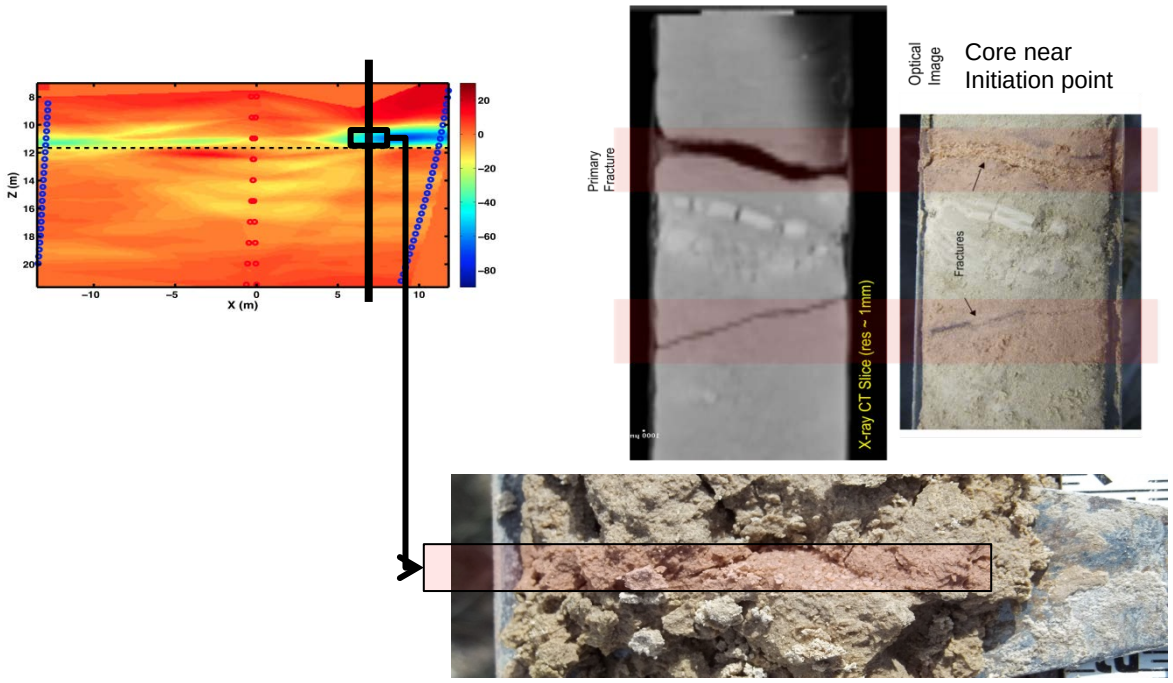

Figure 20. Geophysical estimation of fracture extension.

Top left: Change in seismic signature associated with the fracture (blue) zone. Right: verification of geophysically-detected fractures was performed through core analysis, including x-ray CT imaging (gray image, middle top), slab photography (far right), and field characterization (bottom right).

5.4.4 Geophysical Data Interpretation

The seismic, electrical, and validation core data were used to interpret the fracture locations as described above. The seismic tomography, CASSM, and ERT data agreed with the confirmation soil boring data for locations LBNL-2011-SB02 and -SB04; an example of this comparison is shown in Figure 20. Based on such validation, the geophysical data were used to interpret the spatial distribution of the fractures and amendments.

The interpreted outline of the fracture and amendment-impacted regions near the shallow fracture based on our developed geophysical signature understanding are shown in Figure 21(a). The amorphous outlines indicated distributions based on the geophysical data over the regions where those data were collected. The green circle shows the estimated distribution of the fracture if the wellbore geometry had permitted imaging over all regions, based on connecting the farthest points of fracture disturbance that was geophysically detected. This "green circle" assumption has potential for both over and underestimation. The fractures may not have propagated where the geophysical data did not image (thus leading to an overestimation of the fracture disturbance area). However, it is also likely that the fractures continue at distances beyond those indicated by the geophysical data, based on limited geophysical detectability of small factures (thus leading to an underestimation in the fracture disturbance area).

The interpreted distributions based on the assumption that the fractures and amendments are both radially distributed as shown in Figure 21(b). It illustrates that the estimated fracture radius is greater than the initial conceptual model (shown by the red circle) and is offset, and that the

estimated amendment lateral distribution is less than the initial conceptual model (which was equal in extent to the fracture distribution). Not shown but interpreted from the ERT data, is the vertical extent of the amendment distribution, which was greater than the initial conceptual model. Figure 21(b) shows that the centers of the fracture and amendment distribution regions were offset from the fracture initiation point. The combined ERT and seismic data suggest that although a good fracture was not successfully installed in the deeper zone, some porosity enhancement occurred, which enabled the introduction of some amendment into that zone.

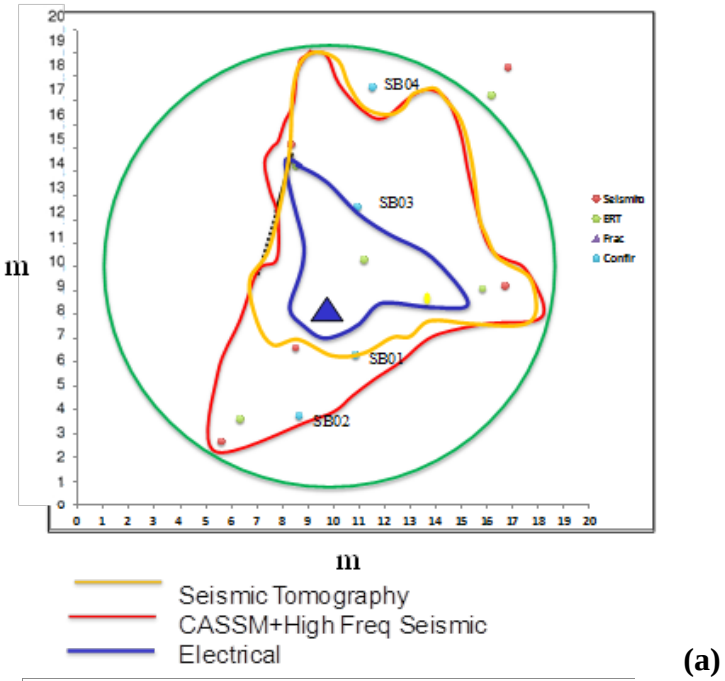

(a)

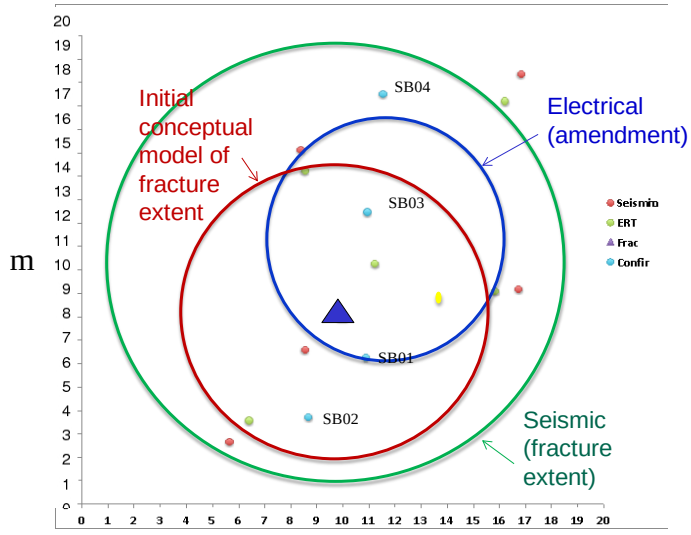

(b)

Figure 5. Interpreted fracture and amendment distributions.

Top: Distribution of fractures and amendments based on geophysical data (yellow, red, and blue outlines), only considering the regions over which seismic data were collected. The green circle indicates the distribution of the installed fracture by assuming that the fracture is radially distributed over the areas that the geophysical data could not image due to borehole geometry.

The blue line indicates the distribution of amendment within the fracture, based on ERT. Bottom: A comparison of the estimated fracture distribution from the geophysical data (green circle, assuming radially distributed) with the distribution used to guide remediation at SS7 (red circle) and the amendment distribution from ERT (blue).

6.0 PERFORMANCE ASSESSMENT

As previously stated, the primary objective of this project is to assess the utility of surface and crosshole geophysical methods for developing a conceptual model of amendment distribution via hydraulic fracturing. Accomplishing this objective is dependent on the quantitative and qualitative performance objectives described below.

6.1 QUANTITATIVE PERFORMANCE OBJECTIVES

The success of the demonstration is dependent on four quantitative performance objectives: 1) confirm fracture characteristics, 2) quantify utility of geophysical methods for delineating fracture and HRC® ROI, 3) assess the value of different geophysical approaches, and 4) determine if there is a cost benefit. These objectives are listed in Table 1 and are described below.

6.1.1 Quantitative Objective #1

The first objective was assessed by evaluating post-fracture installation soil cores to observe fracture characteristics including physical ROI, fracture thickness, and presence of HRC® within the fracture. A physical fracture radius of 7.0 m (23 ft) from the initiation borehole with 2000 pounds installed per fracture was observed. Based on the success criteria listed in Section 3, an observed direct correlation between SS7 and Plume E was achieved.

6.1.2 Quantitative Objective #2

This objective focused on interpretation of the geophysical datasets in terms of the mean radius and variance of the radius of the fractures and HRC® from the injection point as a function of heterogeneity. The data required to assess this criteria includes the inverted time-lapse field geophysical datasets, interpreted with consideration of the laboratory experimental results and validated using the confirmation soil core information as is shown in Figure 21. This objective was partially achieved. Different individual geophysical datasets were used to estimate the mean horizontal distribution of the fractures (between 7.0 and 9.1 m [23 and 30 ft]), and combinations of data were also used to increase confidence in the interpretation. ERT data were used to estimate the vertical and mean radius (5.2 m [17 ft]) of injected amendment. However, because different geophysical datasets offered different quality of information (refer to Section 6.1.3), we choose to use a scenario approach for input to the cost-benefit analysis rather than estimating a variance associated with a single measurement approach only.

6.1.3 Quantitative Objective #3

This objective focuses on assessing the value of different geophysical approaches for guiding development of amendment delivery strategy. As indicated in Table 5, comparison of geophysical data with wellbore validation data allowed us to assess the relative value of the different approaches for monitoring fractures and amendment. The high frequency tomographic and CASSM methods were most useful for identifying the fracture characteristics (spatial distribution and fracture propagation details, respectively), while the 2D crosshole ERT were most useful for providing information about amendment distribution.

Table 5. Summary of geophysical method performance.

	Method	Hypothesis	Detection?	Utility?
Seismic	High-frequency P-wave seismic ★	Decrease in Vp, Increase in 1/Qp	Decrease in Vp clear, artifacts exist	Spatial distribution of fractures
Seismic	ML-CASSM ★	Decrease in Vp, Increase in 1/Qp	Decrease in Vp, small increase in attenuation	Fracture propagation detail
Electrical	Surface ERT ~	Increase in conductivity	Time-lapse corrupted by changes in soil moisture (etc)	Not useful for monitoring but useful for baseline characterization
Electrical	Borehole ERT (2D) ★	Increase in conductivity	Decrease in resistivity, some anomalies	Amendment distribution
Electrical	Combined 3D ERT ~	Increase in conductivity	Decrease in resistivity, some anomalies.	Amendment distribution

Notes:
The red stars indicate the methods that were deemed to be most useful for monitoring the fracture emplacement and subsequent amendment distribution. The "~" symbols indicate that the method was not prioritized as high potential out of the suite of methods tested.
ML-CASSM = multi-level continuous active source seismic monitoring
Qp = Seismic P-wave quality factor (inverse of attenuation)
Vp = Seismic P-wave velocity

Quantitative performance success is dependent on whether the use of geophysics can reduce the number of fracture initiation points by 20%. The value-added in the use of geophysical methods was evaluated by assessing/comparing two situations. The first situation considers only historical site data and soil boring data, and the second situation evaluates the use of the geophysics datasets.

Although fracture ROIs have been observed to vary somewhat across FEW, soil cores collected from SS7 and other FEW plumes indicated that 2000 pounds of proppant material reproducibly creates fractures with radii of approximately 5.2 to 7.0 m (17 to 23 ft) from the initiation point, or an average of a 6.1-m (20-ft) physical fracture radius. Based on the field-scale pilot tests conducted at both SS7 and Zone C, a 6.1 m (20 ft) ROI was chosen as the standard design for the demonstration site (Plume E). Two scenarios were evaluated for this performance and cost assessment, a conservative ROI of 7.0 m (23 ft) and the more probable ROI of 7.6 m (25 ft). Scenario 1 and 2 were evaluated for four different treatment zone areas (1, 4, 8, and 20 acre sites) and compared to the standard design ROI of 6.1 m (20 ft). For each treatment zone area, the number of initiation points was determined for each ROI by dividing the total treatment zone area by the impact area associated with the ROI assuming a circular distribution. The percent difference between the standard design and the Scenario 1 and 2 designs was then calculated. Results for both scenarios are included in Table 6 and Table 7.

Both Scenarios 1 and 2 achieved at least a 20% reduction in the number of fracture initiation points as required by the performance criteria.

Table 6. Performance evaluation: Scenario 1.

Treatment Zone (acres)	1.0	4.0	8.0	20.0
Number of initiation points (20 ft ROI)	35	139	277	694
Number of initiation points (23 ft ROI)	27	109	217	544
% Difference (decrease)	-21.6%	-21.6%	-21.6%	-21.6%

ROI = radius of influence

Table 7. Performance evaluation: Scenario 2.

Treatment zone (acres)	1.0	4.0	8.0	20.0
Number of initiation points (20 ft ROI)	35	139	277	694
Number of initiation points (25 ft ROI)	22	88	175	438
% Difference (decrease)	-36.8%	-36.8%	-36.8%	-36.8%

6.1.4 Quantitative Objective #4

The cost-effectiveness of geophysical imaging relies upon both the cost of technologies used and quality of data obtained. The cost-benefit analysis included: 1) interpretation of qualitative and quantitative performance objectives using integrated geophysical and soil core sample analysis; 2) cost of the dynamic pilot test and associated interpretation; and 3) actual costs associated with the SS7 full-scale RA using a design strategy based on conventional soil core- and groundwater monitoring-based methods alone. Based on the SS7 remedial design and potential treatment zone size, the number of installed fractures was estimated for both Scenarios 1 and 2 for each evaluated treatment zone area. Using a per fracture cost developed from the actual SS7 RA cost, the total cost of implementation was estimated and compared to the cost of the standard design. For Scenario 1, geophysics is only a viable option for larger sites, greater than 20 acres. For Scenario 2, geophysics was found to be viable for treatment zone areas greater than 4 acres. Complete results, further details, and assumptions relating to the cost benefit are included in Section 7.

6.2 QUALITATIVE PERFORMANCE OBJECTIVES

The success of the demonstration is dependent on four qualitative performance objectives, which are to: 1) determine which geophysical method provides the best information about fracture delineation, 2) determine which geophysical method provides the best information about HRC® distribution, 3) determine which geophysical datasets are optimal for monitoring both fracture creation and HRC® distribution, and to 4) assess field ruggedness, required user experience, and

overall signal-to-noise ratio of commercially available geophysical approaches for monitoring HRC® and fracture distribution.

6.2.1 Qualitative Objective #1

After a careful examination of the acquired datasets, the two modalities of high-frequency time-lapse seismic datasets were deemed to provide the best information concerning fracture location. Both the P-wave seismic and CASSM acquisition methods located and spatially mapped the upper fracture zone; estimated fracture depths matched well with both drilling logs from fracture emplacement and fracture location estimated from confirmation boreholes. While both seismic acquisition methods provided equivalent results in the post-fracture period, the CASSM dataset provided both better time resolutions during the fracturing process and more repeatable waveforms; this combination of factors increased our confidence during the interpretation process.

6.2.2 Qualitative Objective #2

Despite the success of the seismic imaging approaches in determining the fracture locations, neither interpreted seismic dataset (seismic velocity or attenuation alteration) provided definitive information concerning HRC® distribution within the emplaced fracture. This is not surprising considering that the seismic response is due to mechanical alteration (introduction of the fracture/proppant system) and the fluid added to the proppant is probably a secondary effect. The most informative dataset for estimating HRC® distribution appeared to be the borehole ERT dataset, which effectively captured the guar breakdown process and HRC® diffusion into the formation.

6.2.3 Qualitative Objective #3

No single geophysical technique allowed simultaneous mapping of both fracture extent and amendment distribution with a high degree of confidence. This observation suggests that multi-method acquisition would be the most effective approach for achieving this qualitative objective. Considering that both borehole ERT and seismic instrumentation can be effectively co-located in monitoring wells, a possible solution might be co-instrumentation with CASSM and borehole ERT to capture separate processes from a similar geometry. This seismic/ERT co-instrumentation approach is currently being adopted for deep monitoring systems used to map subsurface CO_2 movement (Hovorka et.al., 2011).

6.2.4 Qualitative Objective #4

Of the techniques evaluated, borehole ERT is the most mature when applied to environmental monitoring tasks. Commercial vendors can supply the acquisition electronics and turn-key processing packages allowing wide deployment of the technique with minimal training required. Campaign high-frequency seismic acquisition systems are also available commercially but are somewhat more complicated to deploy; also, a key component of the data processing flow (travel-time picking) is a manual process and requires a reasonable degree of training to effectively perform. The CASSM technique, while robust, is currently not commercially available as a system although the majority of the components can be purchased from commercial sources. The processing of CASSM datasets is also more time consuming due to the large data volume of a typical acquisition run (i.e., orders of magnitude larger than traditional

campaign seismic acquisition). At the present time, a combination of borehole ERT and campaign high-frequency seismic acquisition may be the best choice considering training and equipment requirements; however, the CASSM system utilized in this project would be relatively straight-forward to commercialize (both acquisition and processing), a process which make this technique available to a broader community.

7.0 PERFORMANCE ASSESSMENT

7.1 COST MODEL

A cost model for the use of geophysical imaging to investigate the delivery of amendments in the subsurface is provided in Table 8. The table identifies specific cost elements, the data tracked corresponding to the cost elements, and the associated costs. Because this demonstration is based, in part, on the SS7 RA, the actual costs for implementing the RA are also included.

In developing the cost model, it was assumed that only the drilling, biostimulation, and bioaugmentation cost elements were impacted by a change in ROI and, therefore, the number of fracture initiation points. In Table 8, the drilling, biostimulation, and bioaugmentation costs to implement the geophysical methods are presented on a cost per fracture basis. Drilling costs include the drilling subcontractor, IDW disposal, surveying, and labor; prorated based on the number of new monitoring wells and confirmation soil borings installed in each groundwater zone. Biostimulation costs include subcontractors and materials (HRC®, fracture sand, guar, and other fracturing related materials), equipment rental, and labor associated with hydraulic fracturing activities. Biostimulation costs are prorated based on number of fracture initiation locations installed in each groundwater zone. Bioaugmentation activities costs include the pneumatic injection subcontractor, microbial culture materials (e.g., KB1TM), and labor; prorated based on the number of bioaugmented injection wells in each groundwater zone).

Certain cost elements in the cost model are assumed to be constant for a full-scale implementation and not dependent on changes in fracture ROI. These cost elements include the remedial design, groundwater monitoring, project management, geophysical capital and labor, and site closure activities. These are reflected as “Non-Impacted Costs” in Table 8. Groundwater monitoring costs are prorated based on the number of performance monitoring wells in each groundwater zone.

Table 8. Cost model.

Cost Element	Data Tracked	Estimated Cost
Actual Costs to Implement Full-Scale RA at FEW SS7 - Shallow Groundwater Zone		
Remedial Design**		$ 596,325.00
Drilling Activities*	Monitoring Well Installation	$ 11,645.50
	Confirmation Soil Borings	$ 55,882.50
	IDW	$ 18,192.50
	Surveying	$ 9,792.50
Groundwater Monitoring Activities	Groundwater Monitoring	$ 146,304.00
	Analytical Data Validation	$ 8,487.00
	Monitoring Report	$ 15,028.00
Biostimulation Activities*	Mobilization/Demobilization	$ 46,406.50
	Fracturing (Sub and Materials)	$ 1,381,673.50
	Remedial Action Report	$ 32,065.50
	ERPIMS, Database, GIS	$ 6,018.50
Bioaugmentation Activities*	Remedial Design Update	$ 33,704.00
	Pneumatic Injection (Sub and Materials)	$ 177,031.00
Project Management Activities	Project Management	$ 107,337.00
	Meetings	$ 33,200.00
Site Restoration and Close-Out**		$ 28,553.00
Total (Shallow Groundwater)		**$ 2,707,646.00**
Estimated Costs to Implement Geophysical Methods		
Remedial Design**		$ 596,325.00
Geophysics (CASSM)	Capital Costs, labor, mobilization, data interpretation	$ 104,000.00
Drilling Activities* per Fracture	Monitoring Well Installation	$ 18.22
	Confirmation Soil Borings	$ 87.45
	IDW	$ 28.47
	Surveying	$ 15.32
Groundwater Monitoring Activities	Groundwater Monitoring	$ 146,304.00
	Analytical Data Validation	$ 8,487.00
	Monitoring Report	$ 15,028.00
Biostimulation Activities* per Fracture	Mobilization/Demobilization	$ 72.62
	Fracturing (Sub and Materials)	$ 2,162.24
	Remedial Action Report	$ 50.18
	ERPIMS, Database, GIS	$ 9.42
Bioaugmentation Activities* per Fracture	Remedial Design Update	$ 52.74
	Pneumatic Injection (Sub and Materials)	$ 277.04
Project Management Activities	Project Management	$ 107,337.00
	Meetings	$ 33,200.00
Site Restoration and Close-Out**		$ 28,553.00
Total Per Fracture Cost*		**$ 2,773.73**
Number of Fractures		**1**
Non-Impacted Costs (Shallow Groundwater)		**$ 1,039,234.00**
Total (Shallow Groundwater)		**$ 1,042,007.73**

Notes:
*Activities impacted by number of fracture initiation points.
**Cost included based upon Final Record of Decision (ROD), 2006a
IDW = investigation derived waste
ERPIMS = Environmental Resource Program Information Management System
GIS = Geographic Information System

7.2 COST DRIVERS

Potential cost drivers that should be considered when selecting geophysical imaging for developing a conceptual model of fracture propagation and amendment distribution include the size of the treatment area and site geology.

When using geophysical methods like CASSM, the cost to purchase the necessary equipment can be a large percentage of the implementation cost, especially for smaller treatment zones. As shown in this demonstration, geophysical imaging was not a financially viable option for 1-acre treatment sites. Financial practicality at average-sized sites (e.g., 4 to 8 acres) was dependent on the potential fracture impact area, which may be influenced by geology.

As described in Section 5, site geology may impact fracture propagation, and therefore, treatment success. The use of geophysical methods can help identify fracture installation and confirm or supplement soil boring observations early in the remediation process. For this study, the intermediate aquifer zone fracture did not propagate as expected and instead may have moved up into the shallow fracture following a path of least resistance. The use of geophysical methods identified this issue early on. If implemented during a field-scale RA, early identification can allow for timely corrective actions to ensure effective treatment and potentially reduced risk of remediation failure or additional costs.

7.3 COST ANALYSIS

Because the cost-benefit analysis for development of an amendment delivery strategy using geophysical data is based on the implemented SS7 full-scale RA, it was important that the pilot test be as similar as possible to the RA implemented at SS7. To document fracture characteristics for comparison to other FEW areas, each fracture was evaluated using traditional confirmation soil boring methods and compared to previously collected data. Soil cores collected from SS7 and other FEW plumes indicated that 2000 pounds of proppant material reproducibly creates fractures with radii of approximately 5.2 to 7.0 m (17 to 23 ft) from the initiation point, or an average of a 6.1-m (20-ft) physical fracture radius. As stated in Section 6, a 6.1 m (20 ft) ROI was chosen as the standard design for comparison to geophysical methods at Plume E. The pilot test was designed with geophysical data wells installed to image fractures with a radius of 4.6 to 9.1 m (15 to 30 ft) from the initiation point.

Using the actual RA costs from SS7 (Table 8), a per fracture cost was estimated to be $2774. It was assumed that the site geology was consistent throughout the entire treatment zone, regardless of size. This assumption limited the number of pilot tests to one, and therefore, one unit cost for geophysical methods. Because the cost analysis was evaluated using a per fracture cost, another assumption was that the fracture implementation would be similar to the remedial design for SS7. For example, at SS7 each fracture initiation point had 4, 5, or 6 fractures installed. Within the 400 parts per billion (ppb) contour of SS7, 37.5% of the fracture initiation points had four fractures, 25% had five fractures, and 37.5% had six fractures. This same methodology was used for each treatment zone area evaluated to determine the total number of fractures installed. It was also assumed that, based on the CASSM and ERT dataset results, only CASSM would be chosen for use during a field-scale pilot test. Amendment is not likely to distribute laterally beyond the fracture. Based on the success at SS7, it is anticipated that the bacteria will grow, or "bloom," away from delivery zones as aquifer conditions are established by migrating amendment materials, potentially creating bioactivity zones between delivery points over time.

In situ bioremediation application, such as the RA implemented at SS7, have excelled in fine-grained, slow moving groundwater conditions where hospitable geochemical conditions (e.g., adequate and available food source) have been established, with native microbes "blooming" up to 21.3 m (70 ft) from amendment delivery locations. For this reason, it is anticipated that geophysical imaging of the fracture propagation is sufficient for remedial design purposes, and therefore, only CASSM costs were incorporated into the cost analysis.

Results of the cost-benefit analysis for Scenarios 1 and 2 are included in Table 9 and Table 10, respectively.

Table 9. Cost-benefit analysis: Scenario 1.

Treatment Zone Area Size	1 acre	4 acres	8 acres	20 acres
Number of Fractures - 20 ft ROI	173	694	1387	3468
Estimated Cost - 20 ft ROI	$480,986	$1,923,942	$3,847,885	$9,619,712
Number of Fractures - 23 ft ROI	136	544	1087	2718
Estimated Cost - 23 ft ROI	$480,961	$1,611,844	$3,119,689	$7,643,222
% Cost Savings	0.0%	-16.2%	-18.9%	-20.5%

Table 10. Cost-benefit analysis: Scenario 2.

Treatment Zone Size	1 acre	4 acres	8 acres	20 acres
Number of Fractures - 20 ft ROI	173	694	1387	3468
Estimated Cost - 20 ft ROI	$480,986	$1,923,942	$3,847,885	$9,619,712
Number of Fractures - 25 ft ROI	110	438	876	2190
Estimated Cost - 25 ft ROI	$407,775	$1,319,101	$2,534,202	$6,179,505
% Cost Savings	-15.2%	-31.4%	-34.1%	-35.8%

From these results, it is evident that for Scenario 1 (7 m [23 ft] ROI), the use of geophysics to achieve a 20% cost savings is only a viable option for larger sites (greater than 20 acres). For Scenario 2, (7.6 m [25 ft] ROI), the use of geophysics to achieve a 20% cost savings was found to be viable for treatment zones greater than 4 acres, generating a cost savings greater than 30% for the three treatment zone sizes evaluated.

Due to similar site lithology and contaminant distribution, it is anticipated that Plume E will be impacted by the implemented RAs the same way as SS7. As identified in the ROD, the timeframe for SS7 to meet RAOs is estimated at 35 years for the shallow aquifer zone and 175 years for the intermediate aquifer zone (USAF, 2006a). As of the March 2009 performance monitoring conducted at SS7, the updated groundwater model results indicate that MCLs may be reached in the shallow aquifer zone approximately 25 to 30 years after bioremediation initiation. Considering bioremediation was initiated in 2006, MCLs in the shallow aquifer zone are estimated to be reached in 2036 or 2037. The model indicates that MCLs may be reached in the intermediate aquifer zone 50 to 55 years after bioremediation initiation, or in 2061.

8.0 IMPLEMENTATION ISSUES

There are several issues that could potentially impact the use of geophysical data to provide high-quality data needed to design a full-scale remedial treatment. The first issue is the thoughtful design of the pilot study site, which should take into consideration the (often limited) propagation characteristics of the different geophysical signals, expected fracture distribution and costs of drilling wellbores for geophysical data acquisition. Not surprisingly, this study found that in areas where wellbore placement resulted in good geophysical signal coverage the fracture and amendment distribution could be estimated with high confidence, but that certainty was lower elsewhere. Although trade-offs between wellbore spacing, cost, geophysical coverage, and resolution cannot be circumvented, they do require thoughtful consideration during planning.

Another issue is the role of heterogeneity on fracture propagation characteristics. The demonstration was designed to test and image induced fracture characteristics in two different lithologies. The geophysical data in fact illustrated that the team was unsuccessful at installing fractures in one of the lithologies. Although these results highlight the value of geophysical monitoring for understanding fracture distribution as a function of heterogeneity, they also emphasize the need to also consider the geology carefully during pilot study and full-scale design of fracture-based treatment.

The last implementation issue identified was related to the procurement of one of the geophysical methods tested in this demonstration. All but one of the methods are commercially available. However, the CASSM system was developed at LBNL, and therefore, is not commercially available. However, fabrication of the system is not onerous – it can be built by interested geophysical service providers and used to provide a unique and useful service. As such, the fabrication costs-benefit that involved the use of CASSM was included as a fracture monitoring tool.

9.0 REFERENCES

Ajo-Franklin, Jonathan et al. “Applying Compactness Constraints to Differential Travel Time Tomography." *Geophysics* 72, no. 4 (2007): R67-R75.

Ajo-Franklin, Jonathan et al. “Multi-level Continuous Active Source Seismic Monitoring (ML-CASSM): Mapping Shallow Hydrofracture Evolution at a TCE Contaminated Site” (Abstract presented at the annual meeting of SEG, San Antonio, TX, September 18–23, 2011).

Daley, T.M. et al. “Continuous Active-Source Seismic Monitoring of CO_2 Injection in a Brine Aquifer.” *Geophysics* 72, no. 5 (2007): A57-A61.

Daley, T.M., Jonathan B. Ajo-Franklin, C. Doughty. “Constraining the Reservoir Model of an Injected CO_2 Plume with Crosswell CASSM at the Frio-II Brine Pilot.” *International Journal of Greenhouse Gas Control* 5, no. 2 (2011): 1022-1030.

Hovorka, S.D. et al. “Monitoring a Large Volume CO_2 Injection: Year Two Results from SECARB Project at Denbury’s Cranfield, Mississippi, USA.” *Energy Procedia* 4 (2011): 3478-3485.

Hubbard, S.S. et al. “Geophysical Monitoring of Hydrological and Biogeochemical Transformations Associated with Cr(VI) Biostimulation.: *Environmental Science and Technology* (2008): DOI 10.1021/es071702s.

Lawrence Berkeley National Laboratory. *Demonstration Plan: Geophysical Imaging for Investigating the Delivery and Distribution of Amendments in the Heterogeneous Subsurface of the F.E. Warren Air Force Base*. 2010.

Revil, A., and P.W.J. Glover. “Theory of Ionic Surface Electrical Conduction in Porous Media.” *Physics Review* 55 (1997): 1757–1773.

Revil, A., and P.W.J. Glover. “Nature of Surface Electrical Conductivity in Natural Sands, Sandstones, and Clays.” *Geophysical Research Letters* 25/5 (1998): 691–694.

U.S. Air Force (USAF). *Final Zone D Groundwater Remedial Investigation Report, F.E. Warren Air Force Base, Wyoming*. 2003.

U.S. Air Force. *Record of Decision, Zone D Groundwater, F.E. Warren Air Force Base, Cheyenne, Wyoming*. 2006a.

U.S. Air Force. *Final Zone D Source Areas Remedial Investigation Report, F.E. Warren Air Force Base, Cheyenne, Wyoming*. 2006b.

APPENDIX A

POINTS OF CONTACT

Point of Contact	Organization	Phone Fax E-Mail	Role In Project
Robert Kelley	ARS Technologies, Inc. 4813 Hyacinth Court Plainfield, IL 60586-8668	Phone: 732-253-8131 Fax: 732-296-6625 E-Mail: bk@arstechnologies.com	Principal Investigator
Susan S. Hubbard	Lawrence Berkeley National Laboratory 1 Cyclotron Road MS 90-1116 Berkeley, CA 94720	Phone: 510-486-5266 E-Mail: Sshubbard@lbl.gov	Co-Principal Investigator
Belinda Butler-Veytia	URS Corporation 8181 East Tufts Avenue Denver, CO 80237	Phone: 303-694-2770 Fax: 303-930-6080 E-Mail: belinda_butler-veytia@urscorp.com	Co-Principal Investigator
Andrea Leeson	ESTCP Office 4800 Mark Center Drive Suite 17D08 Alexandria, VA 22350-3600	Phone: 571-372-6398 E-Mail: Andrea.Leeson.civ@mail.mil	Environmental Restoration Program Manager

ESTCP Office
4800 Mark Center Drive
Suite 17D08
Alexandria, VA 22350-3605
(571) 372-6565 (Phone)
E-mail: estcp@estcp.org
www.serdp-estcp.org